The Effect of Stroke Rate and Intensity on Ergometer Rowing Efficiency

Data Analysis and Modelling

Jeroen Groot

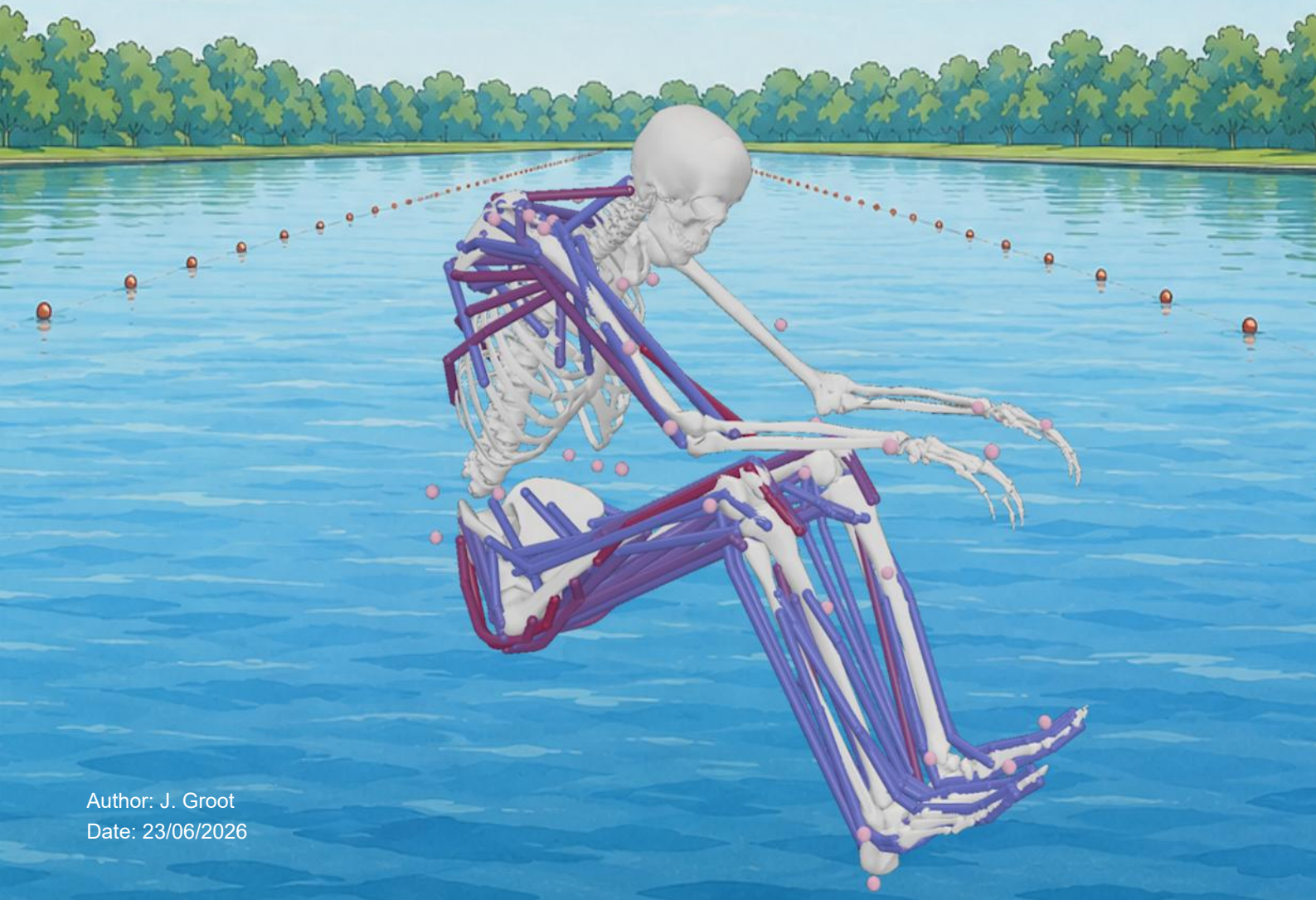

Author: J. Groot
Date: 23/06/2026

The Effect of Stroke Rate and Intensity on Ergometer Rowing Efficiency

Data Analysis and Modelling

By

Jeroen Groot

Supervisors: Ajay Seth
Arnoud Greidanus
Faculty: Faculty of Mechanical Engineering, Delft

TU Delft

Preface

This thesis was written as the final project of my master's programme in Mechanical Engineering at Delft University of Technology. The project combined two of my main interests during my years as a student in Delft, mechanical engineering and rowing. Combining two of my interests in one project made it especially exciting for me to work on.

I would like to give special thanks to my supervisors Ajay Seth and Arnoud Greidanus for guiding me through this project. I appreciate all the time and work they have invested in this project, even when they were overloaded with tasks. Their input helped me structure the modelling work and interpret the results more critically. I would also like to thank Simon Loose and Tom van Wouwe for providing the experimental and modelling data on which this thesis was based.

I would also like to thank fellow students and PhD candidates from the Computational Biomechanics Lab for providing feedback, sharing insights and frustrations and just being nice to talk to after or during a long day behind my computer screen.

Finally, I want to thank my family and friends for their support and motivation during this thesis project. Their encouragement helped me stay motivated during the difficult parts of the project. I also want to thank Jara for listening to my worries, providing me with feedback, motivating me and distracting me when I needed it.

Jeroen Groot
Delft, June 2026

Abstract

The effect of stroke rate on metabolic efficiency in rowing is not fully understood. This thesis investigated if deviations from the preferred stroke rate (PSR) affect metabolic efficiency during submaximal ergometer rowing and if this effect depends on intensity. Additionally, a musculoskeletal modelling workflow was evaluated by comparing modelled and experimentally measured whole-body metabolic cost. Muscle-level metabolic contributions and activations were analysed to investigate the muscle group demands predicted by the model.

Pre-existing experimental and biomechanical data from twelve experienced male rowers were analysed. The rowers performed two different intensity conditions at 50% and 65% of their two kilometres maximum (2K max) time-trial power output. Among these fixed power outputs, the rowers used three different stroke rate conditions at PSR, PSR-15% and PSR+15%. The experimental metabolic cost was measured using a breathing gas analysis and was normalized by rowing ergometer power output. The modelled metabolic cost was estimated using a musculoskeletal modelling workflow and residual mechanical power was added separately to account for a part of the models' limitations. A manually calibrated fibre type profile was used for the primary analysis and compared with a literature-based profile.

The experimental results show that ergometer output normalized metabolic cost was lower at 65% intensity compared to 50% intensity, indicating higher metabolic efficiency per Watt of ergometer output at the higher submaximal intensity. Across both intensities the results indicate that there is a shallow U-shaped curve relationship between stroke rate and the normalized metabolic cost. At the PSR, metabolic cost was lowest or close to lowest and metabolic cost increased when deviating from PSR. This effect was most apparent at the 65% intensity condition, where PSR+15% produced a statistically significant increase in normalized metabolic cost from PSR. At 50% intensity condition, deviations from PSR resulted in smaller and non-significant changes.

The residual-corrected musculoskeletal modelling workflow reproduced the intensity difference, but not the stroke rate dependent metabolic responses. The model predicted a larger decrease in normalized metabolic cost from 50% to 65% intensity than observed in experimental data. The model predicted a significant stroke rate effect consisting of a gradual increase in metabolic cost from PSR-15% to PSR+15% at both intensities. Therefore, the model did not reproduce the experimental U-shaped metabolic curve or the stronger PSR+15% metabolic penalty at 65% intensity. Residual mechanical power improved the absolute agreement but remained relatively constant across stroke rate conditions and did not explain the experimental response.

The vasti were the largest contributors to muscle metabolic power predicted by the model, and their contribution and mean activation increased with increasing stroke rate, while peak vasti activation decreased. However, neither vasti nor total summed activation squared showed a robust stroke rate effect. These patterns should only be interpreted as predictions of the model instead of actual physiological mechanisms because the model did not reproduce the complete experimental response. The literature-based fibre type profile produced considerably lower metabolic cost estimates than the calibrated profile and slightly changed the predicted stroke rate response.

Overall, the findings support metabolic efficiency as a factor contributing to preferred stroke rate selection, especially at higher intensity. However, the current modelling workflow was not yet able to reliably explain the muscle-level mechanisms underlying this preference. Participant personalized muscle properties, improved muscle recruitment estimation, and a more complete representation of trunk mechanics and whole-body physiological costs may be required.

Contents

1 Introduction

1.1 Rowing, Stroke Rate, and Efficiency

Rowing is a cyclic whole-body movement, wherein athletes repeatedly alternate between a drive phase and a recovery phase (see Figure 1.1). During the drive phase, an athlete generates force through the coordinated extension of their legs, trunk and arms and transfers this force via a handle to the boat or an ergometer to create mechanical power. During the recovery phase, the rower moves forward to the catch position and prepares for the next stroke. At a given power output, rowers can use different stroke rates, but select a preferred stroke rate, that feels natural or comfortable. The rower's performance depends on their ability to produce high mechanical power for an extended period; therefore, metabolic efficiency may be one of the major factors that influences the preferred stroke rate selection and performance.

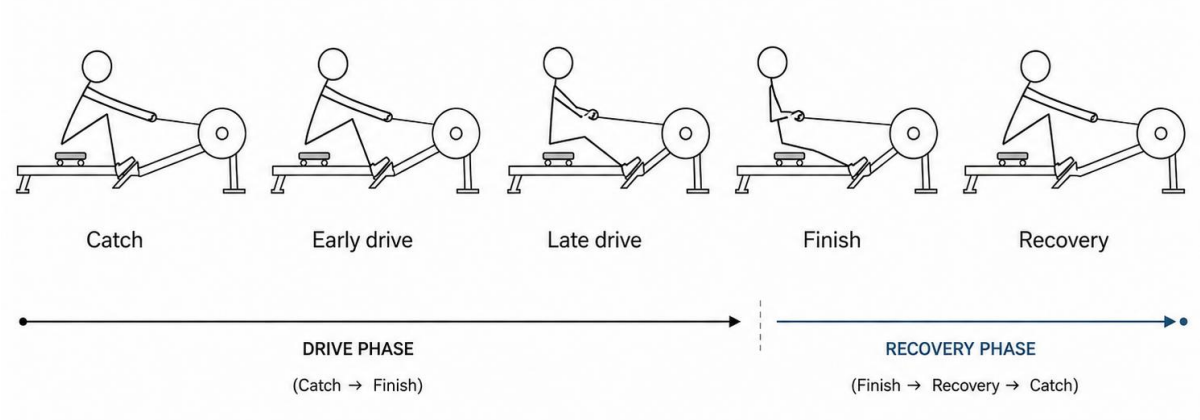

Figure 1.1: *Schematic overview of the ergometer rowing stroke cycle, visually showing the drive phase from catch to finish and the recovery phase from finish to catch.*

1.2 Preferred Movement Frequency in Cyclic Exercise

In other cyclic endurance sports, studies have examined the relationship between movement cycle frequency and efficiency. In running, athletes generally select stride lengths and stride frequencies close to those that minimize metabolic cost. Hunter et al. [1] showed that both experienced and inexperienced runners naturally select stride lengths close to stride lengths that would minimize the use of oxygen, suggesting that minimizing metabolic cost is an important factor in the selection of movement frequency.

In cycling, preferred cadence is often higher than the cadence that minimizes whole-body metabolic cost. Takaishi et al. [2] linked optimal pedalling cadence to the rate of neuromuscular fatigue, suggesting that cyclists may select cadences that balance metabolic economy with preserving local muscle fatigue. Hansen et al. [3] further found that the preferred cadence relates to traits such as muscle fibre type, efficiency, and mechanical optima. Therefore, showing that preferred movement frequency does not necessarily depend on the metabolic efficiency alone.

1.3 Preferred Movement Frequency in Rowing

What determines preferred stroke rate selection in rowing is still uncertain. Hofmijster et al. [4] found there was no significant change in gross efficiency across stroke rates over normal ranges seen in competitive ergometer rowing. This indicates that variations in stroke rate do not have a large impact on efficiency at the group level. However, Ettema et al. [5] found that both stroke rate and intensity influenced several kinematic and kinetic variables, including drive length, drive and recovery times, drive velocity, and work per stroke. At a fixed power output, these stroke rate changes may affect muscle activation, local muscular demand and how work is distributed throughout the body. Therefore, preferred stroke rate selection may represent a balance between metabolic efficiency and muscle-level factors, like in cycling, but this relationship has not been established yet in rowing.

1.4 Musculoskeletal Modelling Purpose

It is possible to evaluate the metabolic cost of rowing with experimental breathing gas analysis. However, it does not provide direct answers about individual muscle contributions to the metabolic cost. This is relevant in rowing because changing stroke rate can change how work is distributed throughout the body. Musculoskeletal modelling can provide additional insight by estimating muscle activations and muscle-level metabolic power based on measured movement data and external forces. This may help determine how stroke rate and intensity influence metabolic cost and which muscle groups contribute to the modelled changes. Also, a musculoskeletal modelling workflow could make it possible to estimate metabolic cost changes for different stroke rates from a rower's movement and force data, without requiring breathing gas data. This could help to analyse rowers' physiological responses to stroke rate and intensity with less equipment.

1.5 Research Aim

Therefore, this thesis investigates if deviations from the preferred stroke rate (PSR) affect metabolic efficiency during submaximal ergometer rowing and if this effect depends on intensity. This is used to evaluate if metabolic cost may help explain the preferred stroke rate selection in rowing. In addition, a musculoskeletal modelling workflow is evaluated by comparing modelled and experimental whole-body metabolic cost. Modelled muscle-level metabolic contributions and activations are also analysed to investigate the muscle-level demands predicted by the model.

It was hypothesized that the lowest normalized metabolic cost would correspond to the PSR. It was also expected that the effect of stroke rate would depend on the intensity of exercise. The musculoskeletal modelling workflow was expected to reproduce the experimentally observed whole-body metabolic response and provide a muscle-level explanation for PSR selection, with lowest activation or metabolic demand at PSR, especially for muscle groups that contribute most to metabolic power.

2 Methods

2.1 Data Acquisition

The experimental data analysed in this research were taken from another study involving male experienced rowers with at least two years of competitive experience [6]. The dataset is complete with biomechanical and physiological information required to perform musculoskeletal simulations and metabolic calculations.

- **Participant characteristics**: The original sample consisted of fourteen male participants (25.31 ± 3.67 years, 189.25 ± 7.93 cm, 83.94 ± 7.48 kg) with a mean two kilometres maximum (2K max) power output of 370.89 ± 63.86 W. Although the original dataset contained 14 participants, two participants were excluded from the present analysis because of incomplete data. The final analysed sample consisted of 12 participants.

- **Experimental research protocol**: Data was collected using a customized Concept2 ergometer at three intensities (50%, 65%, and 75% of average two kilometres (2K) time trial power output) through 7 rowing trials (see Table 2.1); two additional trials were performed at -15% and +15% of the PSR during the trials performed at 50% and 65% intensity.

	Preferred -15%	Preferred stroke rate	Preferred + 15%
50% 2K power	x	x	x
65% 2K power	x	x	x
75% 2K power		x	

Table 2.1: *Experimental data protocol, showing what conditions were measured for each participant.*

- **Kinematic and kinetic data**: The data was recorded from 59 different marker trajectories that were measured by motion capturing of the markers, at a sampling rate of 100 Hz using 14 cameras on the Qualisys tracking system. Data recording for the external forces used three AMTI 6DOF force/torque sensors located under the seat and foot stretchers, at 200 Hz, as well as a 1DOF handle force sensor, at 100 Hz.

- **Physiological Data**:
  - **Electromyography (EMG)**: Surface level EMG was recorded at 2000 Hz from the right side of the body of 14 muscles.
  - **Breathing gas analysis**: The measurement of aerobic energy expenditure associated with each breath was obtained using a Cosmed K5 portable gas analyzer. These data were then used to determine relative net metabolic power consumption during the steady state of the 50% and 65% trials.

- **Musculoskeletal Models**: Pre-scaled musculoskeletal models of each participant have been constructed using a combination of the RajagopalLaiUhlrich lower body model [7] and Seth shoulder model [8] as the basis. The final model includes 26 bodies and 116 muscle-tendon elements.

2.2 Musculoskeletal Model

2.2.1 Model Architecture

The computational framework utilized for this research is a combination of the Rajagopal lower body model [7] and the Seth shoulder model [8] implemented in OpenSim [9], [10], shown in Figure 2.1. This complete musculoskeletal system contains a total of 26 rigid bodies with a total of 47 degrees of freedom to represent the human skeletal system, including pelvis translations and rotations. Additionally, the model incorporates several muscle-tendon elements throughout both lower limbs and in the right upper extremity (totalling 116 muscle-tendon elements), thus including most of the muscles involved during rowing. Because of the implementation of the brachioradialis muscle in the shoulder model, there is a greater degree of physiological accuracy for measuring activations around the elbow joint, since the biceps brachii muscle would be the only major muscle group flexing the elbow joint and therefore would be overestimated in terms of its level of activation, without this incorporation [6].

2.2.2 Skeletal Simplifications

To preserve computational efficiency, several simplifications were made to the model's skeletal geometry [6]. First, the spinal column was modelled as a single rigid body, which does not account for torso bending or spinal flexion during the catch phase of the rowing stroke. The wrist joint was omitted; therefore, the forearm and hand were also represented as a single rigid body with no associated musculature. Consequently, these simplifications have created known sources of kinematic error in the upper body, particularly regarding the tracking of C7 and wrist markers. Specifically, the use of a rigid spine does not allow for the proper tracking of the C7 marker at the beginning of the drive phase (where the rower typically has a bent spine). Also, wrist marker errors may show high levels of variability at the end of the drive phase because the model cannot replicate the ulnar deviation observed at the end of the drive phase as the handle is drawn towards the rower's chest.

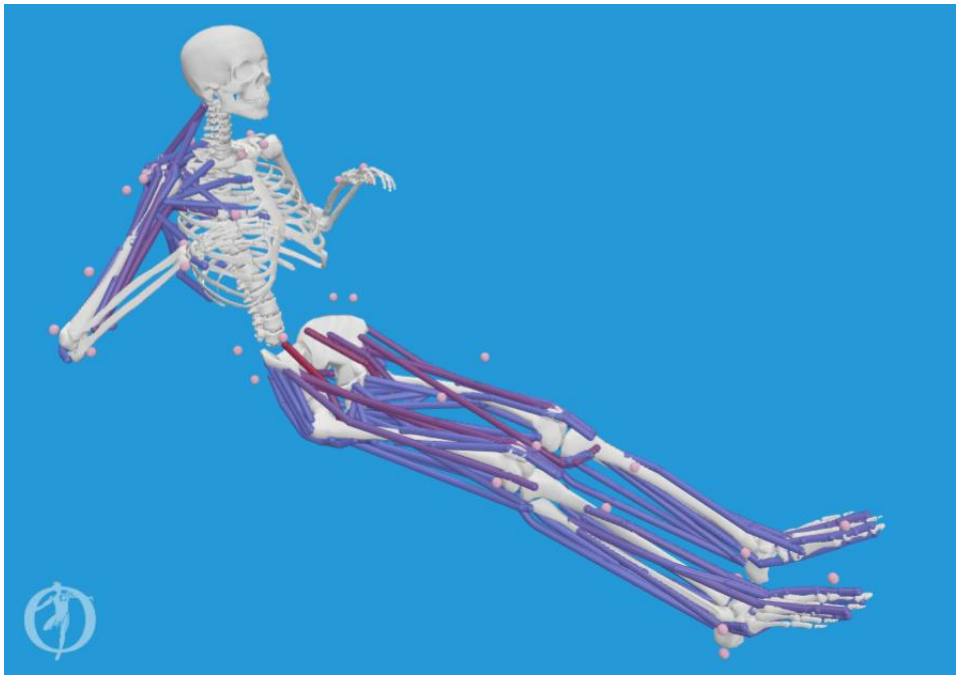

Figure 2.1: *OpenSim model showing model geometry, markers and all muscle segments in a rowing (finish) position.*

2.3 Simulation Pipeline

The data analysis workflow is shown in Figure 2.2. Pre-existing and processed experimental data, Inverse Kinematics (IK) data and scaled musculoskeletal models, gathered from S.V. Loose [6], were used as inputs for the simulation pipeline.

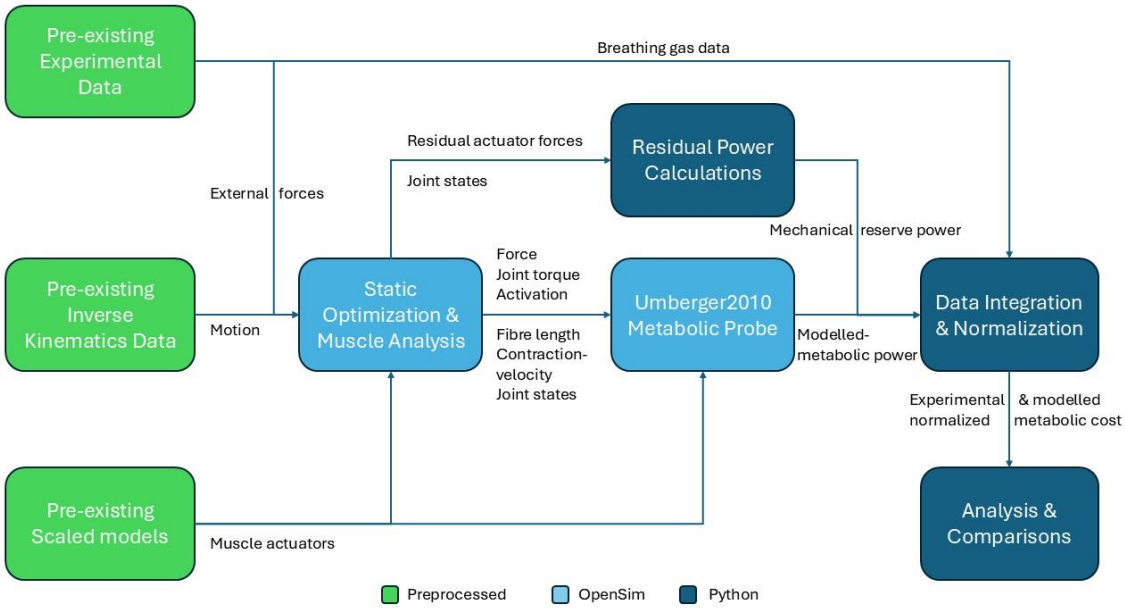

Figure 2.2: *Overview of the workflow used in this study. Pre-existing experimental data, inverse kinematics data, and scaled musculoskeletal models were combined with OpenSim Static Optimization, muscle analysis, Umberger2010 metabolic power estimation, residual power calculation, analysis and comparisons.*

2.3.1 Inverse Kinematics Theory

The tool used to convert the experimental marker trajectories into generalized coordinates for the musculoskeletal model was an IK tool which solves a weighted least squares optimization problem (Equation 2.1). The IK tool uses the experimental marker trajectories and produces a set of generalized coordinate values by minimizing the error between the experimental marker positions and the positions of the virtual markers on the musculoskeletal model. The objective function below describes this optimization problem:

$$\min_{q}\left[\sum_{i\in\text{markers}} w_i \left|\left|x_{exp,i} - x_i(q)\right|\right|^2 + \sum_{j\in\text{coords}} \omega_j \left(q_{exp,j} - q_j\right)^2\right] \tag{2.1}$$

In this expression, q represents the vector of generalized coordinates, $x_{exp,i}$ is the experimental position of marker i, and $x_i(q)$ is the position of the equivalent virtual marker on the model. The term w_i represents the weight which can be assigned to each marker and makes it possible to increase how strongly a marker error is weighted in the error minimization. The second component of the equation describes the minimisation of the coordinate errors between the experimental coordinates $q_{exp,j}$ and model coordinates q_j, weighted by ω_j. This process allows the kinematic description of the modelled rowing stroke to best match the experimental movement performed by the participant.

2.3.2 Static Optimization Theory

SO resolves joint moments (M_j) at every time step by minimizing an objective function based on muscle activations (a_m). This approach uses an assumption that tendons are rigid and that time-dependent muscle dynamics can be neglected. The solver (Equation 2.2) minimizes the sum of squared activations, which penalises high muscle activations and is commonly used as a fatigue-related recruitment criterion:

$$J = \sum_{m=1}^{n} (a_m)^2 \tag{2.2}$$

Subject to the constraint that the joint moment (M_j) must be produced by a corresponding set of muscles, where each muscle produces a force that depends on its activation (a_m), its maximum isometric force $(F_{m,max})$, the length of its muscle fibres (l_m), and the contraction velocity (v_m). The resulting muscle force produced by each muscle is then multiplied by the moment arm corresponding to each muscle's moment arm relative to the joint $(r_{m,j})$. Reserve actuators $(M_{r,j})$ are added to the model to bridge gaps between the required joint moment and the contribution of muscles to this moment (Equation 2.3).

$$\sum_{m=1}^{n} [\, a_m \cdot f(F_{m,max}, l_m, v_m)] r_{m,j} + M_{r,j} = M_j \tag{2.3}$$

After performing the optimization process, a muscle analysis is performed to extract specific physiological variables for each muscle-tendon unit. The primary variables extracted are fibre lengths (l_m) and fibre contraction velocities (v_m). These variables are the mechanical prerequisites required for the Umberger2010 metabolic model [11] to estimate the heat and work outputs of each muscle.

2.4 Metabolic Power Estimation

To estimate the metabolic cost of the rowing stroke, the Umberger2010 metabolic model [11] is used. This model calculates the rate of energy expenditure, at the individual muscle-level, based on the thermodynamic laws for heat production and mechanical work.

2.4.1 Thermodynamic Framework

The total metabolic power $(\dot{E})$ for each muscle-tendon unit is defined as the sum of the heat production rate $(\dot{H})$ and the mechanical work rate $(\dot{W})$:

$$\dot{E} = \dot{H}_{act} + \dot{H}_{maint} + \dot{H}_{short} + \dot{W} \tag{2.4}$$

The terms $\dot{H}_{act}$ and $\dot{H}_{maint}$ refer to thermodynamic heat production associated with muscle activation and with maintaining a muscle in the active state. The shortening heat rate $(\dot{H}_{short})$ describes the energy used during fibre contraction, which is dependent on the contraction velocity (v_m) compared to the maximum contraction velocity (V_{max}). The term $\dot{W}$ is used to describe the rate of mechanical work being performed by a muscle.

2.4.2 Fibre Type Composition and Bhargava Recruitment Strategy

The Umberger2010 model factors in the percentage of slow-twitch (type I) and fast-twitch (type II) muscle fibres and their heat production for each muscle. Type II fibres produce more heat for the same activation as type I fibres, since type II fibres also show a higher ATP consumption rate than type I fibres [12]. The Bhargava recruitment setting [13] was enabled for all simulations. This setting uses fibre type recruitment based on muscle activation. At low activation levels, primarily type I fibres are recruited, while at higher activation levels the recruited composition moves towards the assigned type I and type II fibre proportions.

Two fibre type profiles were evaluated. A manually calibrated profile was used as the primary model configuration. For this profile, the assigned type I fibre percentages were iteratively reduced until the group-level modelled metabolic cost at 50% intensity showed reasonable agreement with the experimental whole-body metabolic cost. A second profile used fibre type percentages based on values from literature [14], [15]. This literature-based profile was used to evaluate how a more physiologically supported fibre type composition affected the modelled results. The assigned fibre type percentages for both profiles are provided in Appendix B (see Table B.1).

2.4.3 Model Basal Rate Configuration

To make the modelled metabolic cost of rowing directly comparable with the experimental data, some settings are applied to the metabolic probe (see Appendix A). The basal metabolic rate, which is the amount of energy needed for basic physiological maintenance at rest, was disabled in the metabolic probe configuration. The experimental breathing gas data were measured so that the basal metabolic rate was measured directly before performing the rowing tasks. The net metabolic rate was calculated by taking the difference between the energy expenditure during rowing (active) and the energy expenditure (resting) measured at baseline pre-trial. Therefore, by performing the simulation without the basal metabolic rate, the energy expenditure in the simulation reflects only the energy expended for rowing and not the energy expended to maintain pre-rowing physiological functions.

2.4.4 Residual Mechanical Power Calculation

The residual actuator outputs from SO were also analysed to estimate extra mechanical power that was not produced by the modelled muscles. The residual power was calculated as actuator force or torque multiplied by the corresponding joint velocity or angular velocity, respectively. The absolute value of residual power was used (Equation 2.5), because both power generation and power absorption by residual actuators mean that the model required non-muscle power.

$$P_{res} = \sum_{i} \left| P_{res,i} \right| \tag{2.5}$$

The Umberger2010 muscle metabolic power and absolute residual mechanical power were summed to obtain the residual-corrected model output (Equation 2.6):

$$P_{model} = P_{Umberger2010} + P_{res} \tag{2.6}$$

When divided by target ergometer power, this quantity is referred to as the normalized metabolic cost. Because the correction includes mechanical residual power, it should not be interpreted as a purely physiological metabolic cost estimate. To determine the strength of the influence of the lumbar extension residual power on the predicted stroke rate response, the residual-corrected model output

was also recalculated after subtracting the absolute lumbar extension residual power. SO was not performed again; therefore, the sensitivity analysis only evaluated the direct contribution of the lumbar extension residual to the correction and did not account for possible redistribution of demand to other modelled muscles.

2.4.5 Data Integration and Normalization

All 116 muscles have their instantaneous metabolic power summed to obtain the whole-body metabolic rate at each time step. Because ten strokes are analysed for each stroke rate condition, the time each stroke takes must be accounted for in the analysis. To obtain mean metabolic power over each stroke, instantaneous metabolic power was integrated over the stroke duration and divided by the stroke cycle time (Equation 2.7):

$$P_{avg} = \frac{1}{T}\int_0^T \sum_{m=1}^{116} \dot{E}_m(t)\, dt \tag{2.7}$$

Because participants differed in 2K maximum power, mean metabolic power was normalized by the measured ergometer power for each condition, corresponding to 50% or 65% of the participant's 2K maximum power. This produced a dimensionless ratio representing the metabolic power required per unit of ergometer output, which was used as the primary efficiency metric. For each participant and condition, values were averaged across the ten representative strokes.

2.4.6 Muscle-Level Metabolic Contribution and Activation Analysis

To investigate the muscle-level responses predicted by the model, the individual muscles were grouped into seven muscle groups: vasti, gluteus maximus, hamstrings, plantar flexors, hip flexors, upper-body pulling muscles, and scapular stabilisers. The muscle elements included in each group are listed in Appendix C (see Table C.1).

The metabolic power of all muscles within a group was summed and averaged over the analysed strokes for each participant. The muscle group contributions were reported both as absolute metabolic power in Watts and as a percentage of the total modelled muscle metabolic power.
The activation outputs from SO were also analysed using the same muscle groups. The activation values of all muscle elements within each group were averaged at each time point. For every stroke, mean activation was calculated as the time-weighted mean of this group activation signal. Peak activation was defined as the maximum value of the group-averaged activation signal. The stroke values were then averaged for each participant and condition. Group-level means and standard deviations were calculated across participants.

Squared activation was also analysed to relate activation results to the objective minimised by SO. At each time point, the squared activation values of all vasti muscle elements were summed to determine the vasti contribution to the activation squared objective. The squared activations of all 116 muscle elements were also summed to determine the total SO activation squared objective. Both signals were time-averaged over each stroke and averaged across strokes for each participant and condition.

2.5 Statistical Analysis

Statistical analysis was performed on the effects of intensity and stroke rate on normalized metabolic cost, which was used as an inverse measure of metabolic efficiency, using a two-way repeated-measures analysis of variance (ANOVA) with intensity and stroke rate as within-subject factors. These analyses were performed for the experimental normalized metabolic cost, modelled normalized metabolic cost, and model error. Model error was defined as modelled normalized metabolic cost minus experimentally measured normalized metabolic cost. Repeated-measures ANOVAs were also performed for vasti peak activation, vasti absolute metabolic power, vasti summed activation squared, and total summed activation squared.

The statistical residuals were examined for normality using Shapiro-Wilk tests, and standardized residuals were screened for outliers. Effects with more than two levels were tested for sphericity. If sphericity was violated, the corrected p value using Greenhouse-Geisser was reported. Generalized eta squared was reported as the effect-size measure. When the residuals deviated from normality, Friedman tests and Bonferroni-corrected Wilcoxon signed-rank comparisons were additionally used to assess stroke rate differences separately within each intensity. The repeated-measures ANOVAs were retained to evaluate the overall intensity effect and the interaction between intensity and stroke rate. An additional sign test was performed for the experimental comparison between PSR and PSR+15% at 65% intensity. The alpha level was set at $\alpha = 0.05$.

3 Results

3.1 Experimental Metabolic Cost and Efficiency

For evaluating the relationship between stroke rate, power output, and metabolic demand, the net metabolic power determined from breathing gas analysis was normalized by the applied target mechanical power output to the erg handle. The resulting metric is the dimensionless amount of metabolic cost to produce one Watt of ergometer handle power.

3.1.1 Group-Level Normalized Metabolic Cost

The analysis of 12 participants' responses to change in both stroke rate and target power output through each of the 12 participants as a group demonstrates different physiological responses to the different conditions as shown in their normalized metabolic cost profiles (Figure 3.1a).

A consistent vertical shift was observed between both target power conditions. The normalized metabolic cost was lower at the 65% intensity condition compared to the 50% intensity condition. For example, at the PSR, the mean normalized metabolic cost dropped from 5.47 ± 0.44 at 50% intensity to 5.22 ± 0.42 at 65% intensity, demonstrating a downward vertical shift. This downward vertical shift indicates a decrease in the normalized metabolic cost at higher submaximal (65%) intensity, thus providing evidence for a greater efficiency at 65% intensity than at 50% intensity of the 2K max power output.

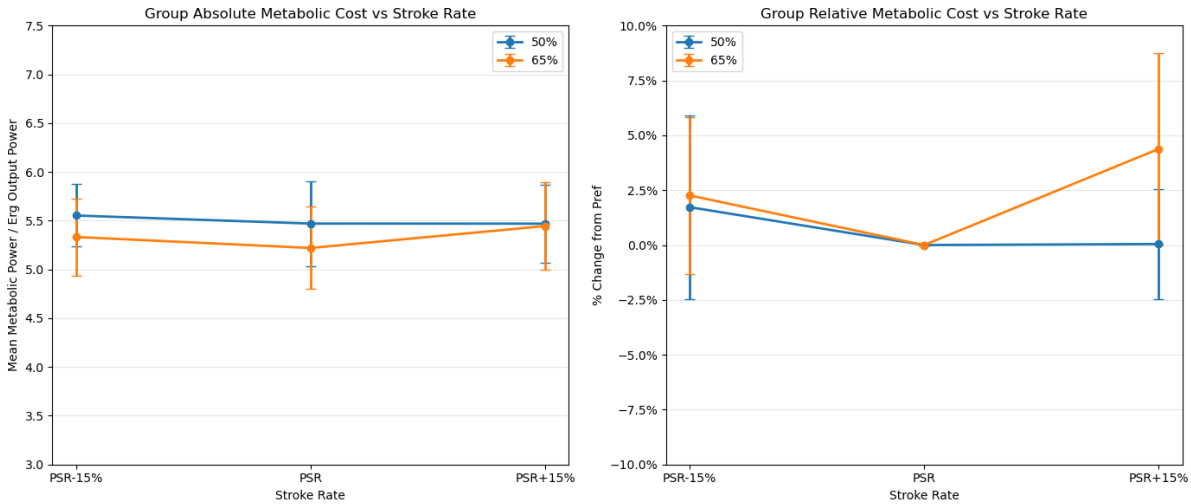

Figure 3.1: *Whole-body experimental net metabolic cost across 12 participants at varying stroke rates (PSR-15%, PSR, PSR+15%) for the 50% (blue) and 65% (orange) of 2K max power conditions.*

- ***(a)*** *The group absolute metabolic cost normalized by target mechanical power (mean ± SD).*
- ***(b)*** *The relative percentage change in normalized metabolic cost calculated using each participant's preferred stroke rate as the zero baseline (mean ± SD).*

3.1.2 Relative Changes from the Preferred Stroke Rate

To show the percentage change in metabolic cost relative to the baseline PSR another graph is shown in Figure 3.1b. An increase in metabolic cost was observed at both workloads when decreasing stroke rate from the PSR. At PSR-15%, the mean metabolic cost increased by 1.73 ± 4.18% for the 50% intensity condition and 2.26 ± 3.57% for the 65% intensity condition. An increase in metabolic cost was observed at both workloads when increasing stroke rate from the PSR. At PSR+15%, the mean metabolic cost increased only slightly by 0.05 ± 2.49% for the 50% intensity condition and a substantial 4.48 ± 4.38% for the 65% intensity condition.

The mean stroke rates at 50% intensity for PSR-15%, PSR and PSR+15% were 17.8, 20.5 and 23.9 strokes/min. At 65% intensity the stroke rates were 20.2, 23.9 and 27.3 strokes/min, respectively. The corresponding participant-level deviations from PSR were -13.2% and +16.9% at 50% intensity, and -15.4% and +14.0% at 65% intensity. Therefore, the stroke rate deviations did not match the prescribed 15% targets perfectly.

3.1.3 Between Participants Variability and Individual Responses

Although the average data from the group appear to describe an overall shallow U-shaped relationship centred around the PSR, the standard deviation error bars show that there is a considerable variation between participants. This variability is further confirmed by an examination of the metabolic profiles for each of the twelve participants shown in Figure 3.2. The absolute vertical heights of the curves vary between subjects indicating individual differences in baseline efficiency. While most participants show a shallow U-shaped curve (especially at 65% intensity output), certain individuals show a flat curve or a decreasing metabolic cost when deviating from the PSR.

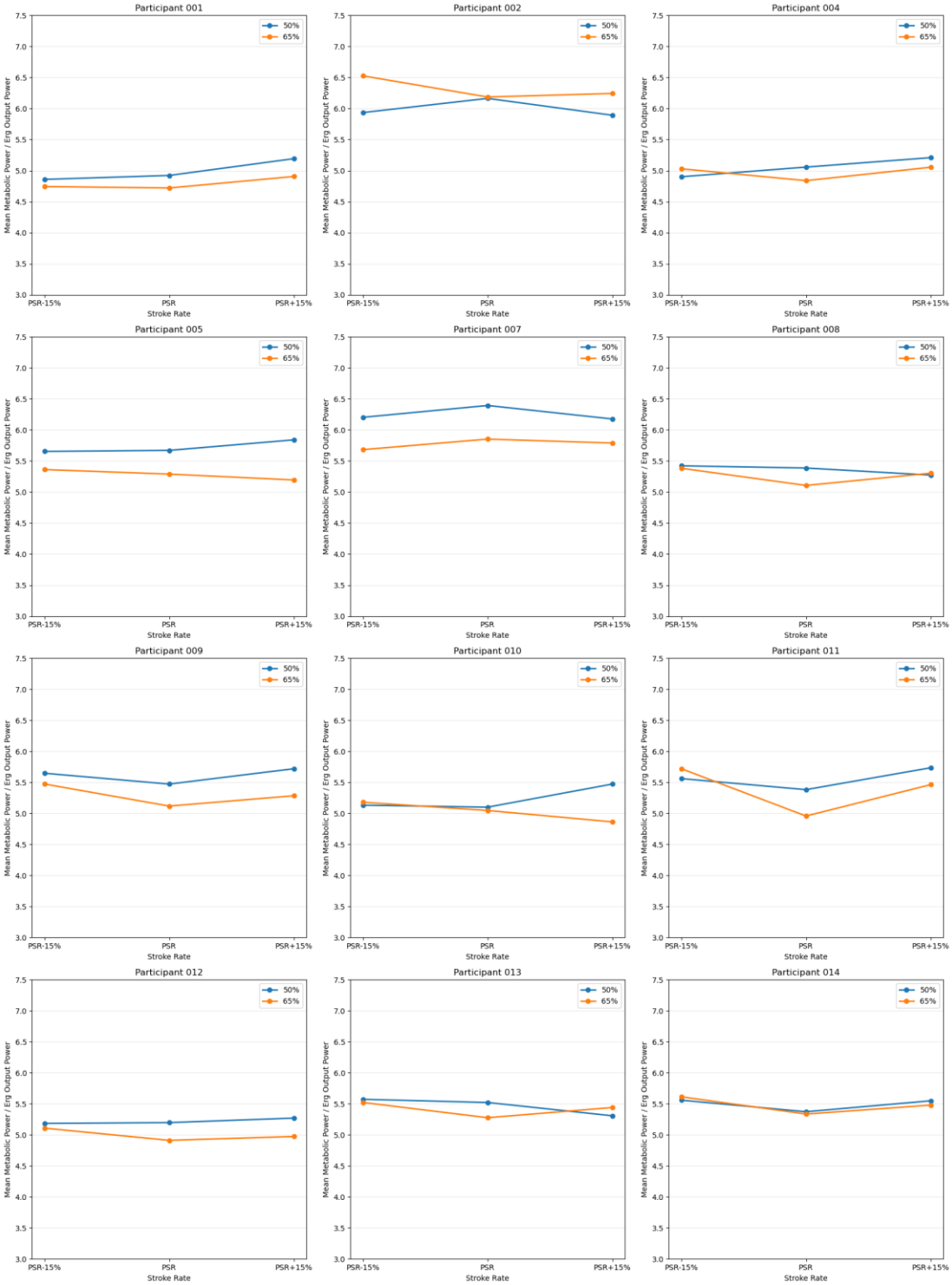

Figure 3.2: *Individual experimental participant profiles showing the normalized metabolic cost across the three stroke rate conditions (PSR-15%, PSR, and PSR+15%). Each of the twelve panels represents a distinct rower ($n = 12$), tracking their specific metabolic response to the 50% target power output (blue line) and the 65% target power output (orange line).*

3.1.4 Statistical Significance of Efficiency Deviations

To determine if the deviations from the PSR were caused by random variation or if they are systematic, a two-way repeated-measures ANOVA was performed on the normalized experimental metabolic cost. Intensities of 50% and 65% of 2K max power, and stroke rates consisting of PSR-15%, PSR, and PSR+15% were the two within-subject factors.

The assumptions of the ANOVA were checked prior to the analysis. All twelve participants provided complete datasets across the six repeated measured conditions. None of the standardized residuals exceeded |3|, indicating no extreme outlier was present. However, Shapiro-Wilk tests on the residuals from the repeated measures indicated a significant deviation from normality (W = 0.945, p = 0.0034). Therefore, the repeated-measures ANOVA results were reported together with non-parametric sensitivity analyses using Friedman tests and Bonferroni-corrected Wilcoxon signed-rank comparisons within each intensity condition.

Analysis	**Effect / comparison**	**Test statistic**	**p value**	**Effect size / direction**	**Interpretation**
Shapiro-Wilk test	Repeated-measures residuals	$W = 0.945$	$p = 0.0034$	—	Residuals deviated from normality
Repeated-measures ANOVA	Intensity	$F(1,11) = 7.32$	$p = 0.020$	$\eta_G^2 = 0.043$	Significant intensity effect
Repeated-measures ANOVA	Stroke rate	$F(2,22) = 4.03$	$p_{GG} = 0.0369$	$\eta_G^2 = 0.016$	Significant stroke rate effect
Repeated-measures ANOVA	Intensity × stroke rate	$F(2,22) = 6.66$	$p_{GG} = 0.0082$	$\eta_G^2 = 0.016$	Significant interaction
Friedman test	Stroke rate at 50% intensity	$Q = 1.17$	$p = 0.558$	—	No significant stroke rate effect
Friedman test	Stroke rate at 65% intensity	$Q = 10.67$	$p = 0.0048$	—	Significant stroke rate effect
Wilcoxon signed-rank test	50%: PSR-15% vs PSR	$W = 25.0$	$p_{bonf} = 0.904$	—	Not significant
Wilcoxon signed-rank test	50%: PSR vs PSR+15%	$W = 39.0$	$p_{bonf} = 1.000$	—	Not significant
Wilcoxon signed-rank test	50%: PSR-15% vs PSR+15%	$W = 21.0$	$p_{bonf} = 0.529$	—	Not significant
Wilcoxon signed-rank test	65%: PSR-15% vs PSR	$W = 15.0$	$p_{bonf} = 0.192$	—	Not significant

Analysis	Effect / comparison	Test statistic	p value	Effect size / direction	Interpretation
Wilcoxon signed-rank test	65%: PSR vs PSR+15%	$W = 4.0$	$p_{bonf} = 0.0103$	11/12 higher at PSR+15%	PSR+15% was higher than PSR
Wilcoxon signed-rank test	65%: PSR-15% vs PSR+15%	$W = 12.0$	$p_{bonf} = 0.103$	—	Not significant
Sign test	65%: PSR vs PSR+15%	11/12 participants higher at PSR+15%	$p_{bonf} = 0.0381$	—	Supported the main Wilcoxon result

Table 3.1: *Statistical summary of the experimental normalized metabolic cost analysis. Repeated-measures ANOVA results are shown together with non-parametric Friedman and Wilcoxon signed-rank tests, because the repeated-measures residuals deviated from normality. Greenhouse-Geisser corrected p values are reported as p_{GG} for effects with more than two levels. Bonferroni-corrected post-hoc p values are reported as p_{bonf}.*

The statistical results are summarized in Table 3.1. The repeated-measures ANOVA showed significant effects of intensity, stroke rate, and their interaction. This indicates that normalized metabolic cost changed between the intensity and stroke rate conditions, and that the stroke rate effect depends on intensity. Post hoc Wilcoxon signed-rank tests, with Bonferroni correction showed a significant difference between PSR and PSR+15% at 65% intensity ($p_{bonf} = 0.0103$). No pairwise comparison was statistically significant at 50% intensity condition. The key comparison of 65% of PSR versus PSR +15% was also supported with a paired difference analysis showing 11 of 12 participants had a higher normalized metabolic cost at PSR +15% than at PSR. Using the sign test, the comparison remains significant after Bonferroni correction ($p_{bonf} = 0.0381$).

These results show that the experimentally measured stroke rate penalty was primarily due to the 65% intensity condition. Rowing at PSR+15% during the 65% intensity condition resulted in a statistically significant increase in normalized metabolic cost when compared to the PSR, while deviations from PSR at 50% intensity were minor and not statistically significant.

3.2 Whole-Body Musculoskeletal Simulation Results

Metabolic cost was estimated using the calibrated profile modelling workflow and compared with the experimental breathing-gas measurements. Residual mechanical power was evaluated separately and added as a correction for mechanical power not produced by the modelled muscles.

3.2.1 Group Normalized Modelled Metabolic Cost Trends

The residual-corrected modelled metabolic power was normalized by the target ergometer power and compared across stroke rate and intensity conditions (Figure 3.3a). At the 50% intensity condition, the model predicted a mean normalized metabolic cost of 5.11 ± 0.47 at PSR-15%, 5.17 ± 0.45 at PSR, and 5.23 ± 0.50 at PSR+15%. At the 65% condition, the corresponding values were lower, with mean normalized metabolic costs of 4.45 ± 0.38 at PSR-15%, 4.54 ± 0.38 at PSR, and 4.60 ± 0.35 at PSR+15%, respectively.

The change that was shown clearest in the modelling data was the vertical separation between the two intensity conditions. For each stroke rate, the model predicted a lower normalized metabolic cost

at 65% than at 50%. At PSR, the normalized cost decreased from 5.17 ± 0.45 at 50% to 4.54 ± 0.38 at 65%. This estimates a reduction between 12 and 13%. While the experimental results also showed a lower normalized cost at 65% intensity, the estimated improvement in efficiency from the modelling data is considerably larger than from the experimental data. This indicates that the residual-corrected model overestimates the improvement in efficiency at the 65% intensity condition.

Within both intensity conditions, the modelled normalized metabolic cost increased gradually from PSR-15% to PSR+15%. Therefore, the model predicted a small consistent stroke rate effect. However, it did not produce the experimental shallow U-shaped response around PSR and only a slightly stronger effect of stroke rate at 65% intensity.

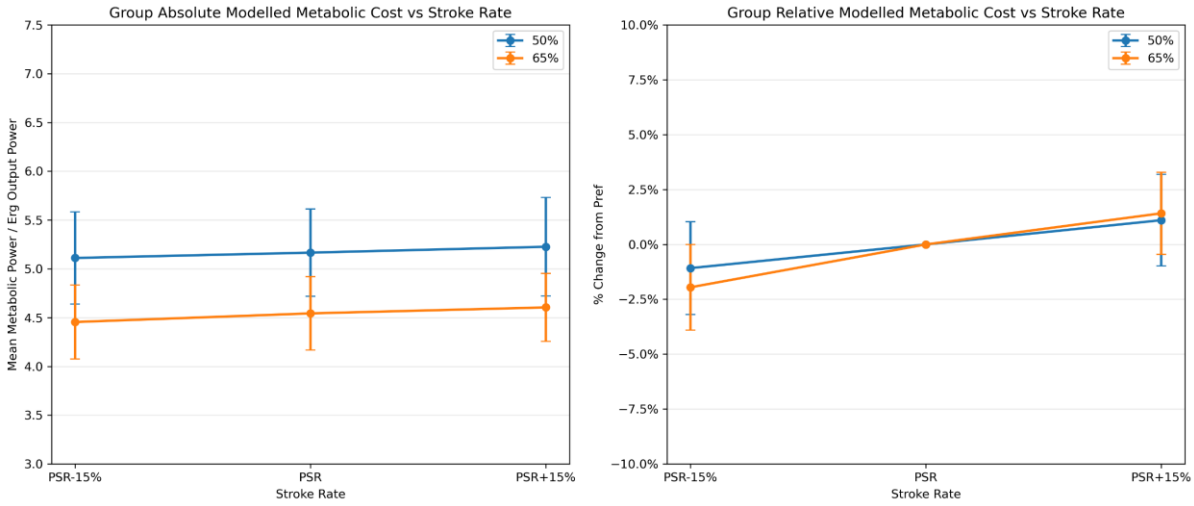

Figure 3.3: *Group-level whole-body modelled normalized metabolic cost, using the calibrated fibre type profile, at varying stroke rates (PSR-15%, PSR, PSR+15%) for the 50% (blue) and 65% (orange) of 2K max power conditions.*

- ***(a)*** *The group residual-corrected metabolic cost normalized by target mechanical power (Mean ± SD).*
- ***(b)*** *The relative percentage change in normalized metabolic cost calculated using each participant's preferred stroke rate as the zero baseline.*

3.2.2 Relative Changes from the Preferred Stroke Rate in the Model

The percentage change in normalized metabolic cost relative to the baseline PSR is shown in Figure 3.3b. The modelled results showed only small relative changes across stroke rate conditions. At PSR-15%, the mean metabolic cost decreased by $1.08 \pm 2.12\%$ for the 50% intensity condition and $1.95 \pm 1.94\%$ for the 65% intensity condition. At PSR+15%, the mean metabolic cost increased by $1.10 \pm 2.09\%$ for the 50% intensity condition and $1.42 \pm 1.87\%$ for the 65% intensity condition. The direction and magnitude of these changes were nearly similar between intensities, which differs from the experimental response where deviations from PSR on both sides resulted in an increase of metabolic cost.

3.2.3 Comparison Between Experimental and Modelled Metabolic Cost

The individual modelled metabolic cost was compared directly to the experimental metabolic cost to evaluate agreement between both datasets. The comparison for absolute metabolic power, both

before and after residual-correction are displayed in Figure 3.4a and 3.4b, respectively. Without residual-correction, the model underestimates the metabolic power, especially at the 65% intensity condition. However, after the mechanical residual power was added, the modelled values shifted closer to the identity line, suggesting a better agreement between the model and experimental data. As for the normalized comparison presented in Figure 3.5a and 3.5b, the model without residual correction was a reasonable fit for part of the 50% intensity condition but consistently underestimated the normalized metabolic cost in the 65% condition. After adding normalized residual power there was a reduction in this underestimation, however differences still existed between subjects.

Figure 3.6 presents group means comparing both the experimental and modelled normalized metabolic cost across stroke rate conditions. The manually calibrated fibre type profile model produced a reasonable estimate of the average metabolic cost at 50%. At 65% intensity, the model predicted lower normalized metabolic cost than was measured experimentally, indicating that the model overestimated the increase in efficiency between the two intensity conditions. In addition, the model did not match the shape of the stroke rate response very well. The experimental data shows a more distinct increase in metabolic cost when deviating stroke rate from PSR, while the modelled curves show a gradual increase in metabolic cost from PSR-15% to PSR+15% at both intensities.

Individual experimental and modelled stroke rate curves are shown in Figure E.1 (see Appendix E). The comparison shows that the model did not consistently produce the same shape as from the experimental response for the participants. Although some of the participants had similar trajectories for the modelled and experimental curves, some of the participants diverged or showed opposite trajectories. Despite residual correction providing improved absolute agreement, it did not reliably reproduce individual-specific stroke rate responses observed in the experimental data.

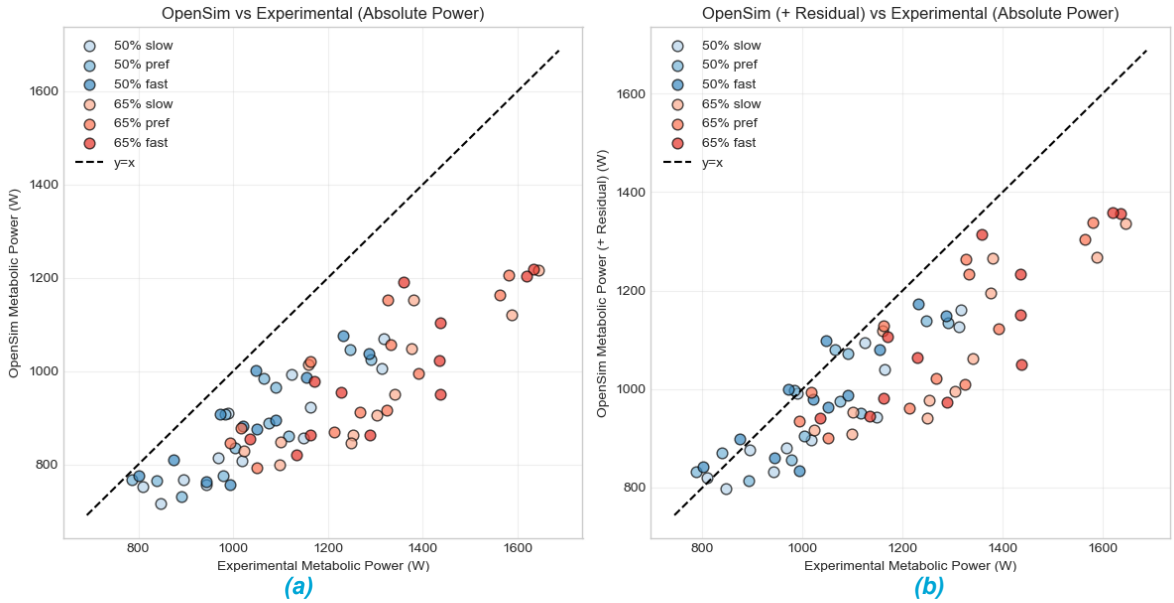

Figure 3.4: *Comparison between experimental and modelled absolute metabolic power.*

- ***(a)*** *Experimental absolute metabolic power compared to modelled muscle metabolic power without residual mechanical power.*
- ***(b)*** *Experimental absolute metabolic power compared to modelled metabolic power with residual mechanical power included.*

The dashed identity line represents perfect agreement between experimental and modelled values.

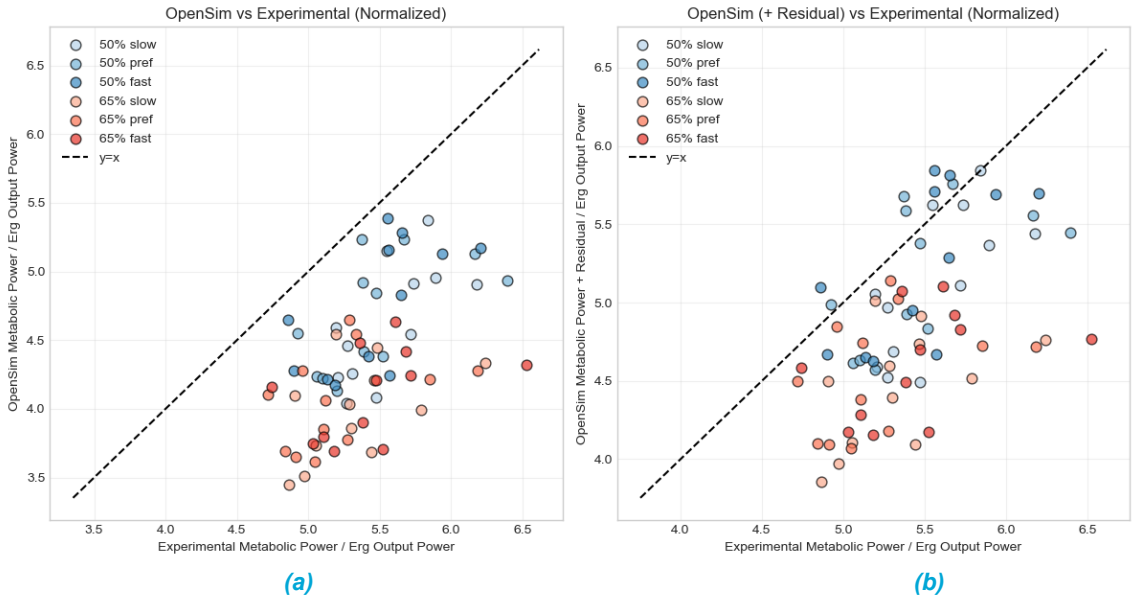

Figure 3.5: *Comparison between experimental and modelled normalized metabolic cost.*

- ***(a)*** *Experimental normalized metabolic cost compared to modelled metabolic cost without residual mechanical power.*
- ***(b)*** *Experimental normalized metabolic cost compared to modelled metabolic cost with residual mechanical power included.*

The dashed identity line represents perfect agreement between experimental and modelled values.

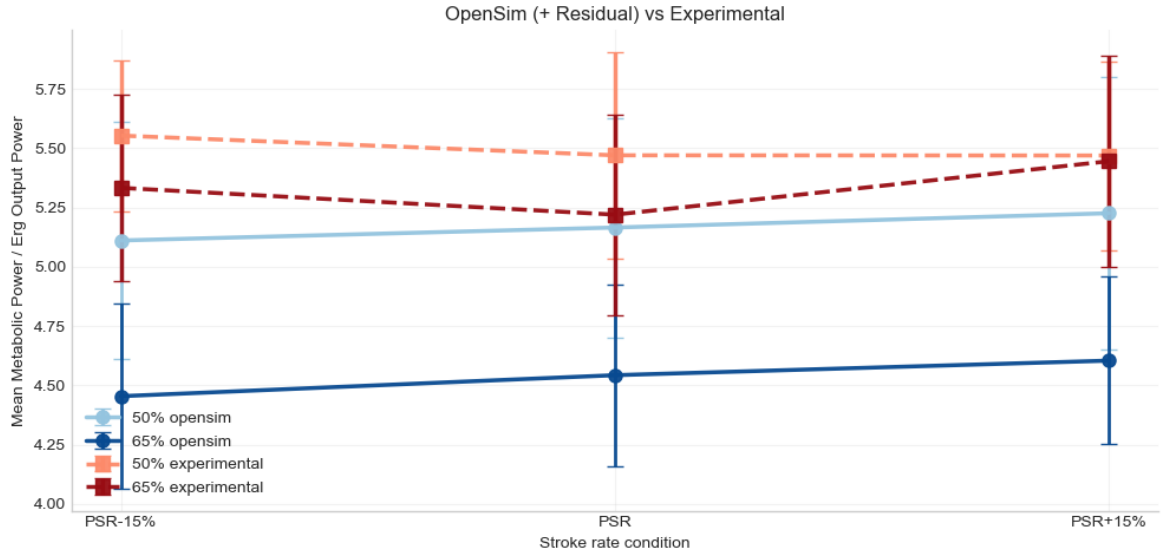

Figure 3.6: *Group mean normalized metabolic cost across stroke rate conditions for experimental breathing gas data and modelled predictions after adding residual mechanical power. Values are normalized by ergometer output power. Error bars indicate pooled standard deviation across participants. Residual correction shifted the modelled values closer to the experimental values, although substantial underestimation remained at 65% intensity.*

3.2.4 Residual Mechanical Power Contribution

The contribution of residuals was analysed separately to assess how much of the residual-corrected metabolic estimate came from non-muscle sources in the model. The residual mechanical power contributed approximately 0.45 to 0.50 times the target ergometer power across different conditions (Figure 3.7). The residual profile was relatively flat across stroke rate conditions and showed almost

no difference between intensity conditions. As a result, residuals mainly contributed as an offset to the modelled metabolic estimate, instead of explaining stroke rate dependent changes.

The residual lumbar extension actuator accounted for almost 50% of the total absolute residual correction and 4 to 5% of the full residual-corrected modelled metabolic cost across all participants and conditions. Excluding this residual contribution reduces the absolute model output but produced almost no change in stroke rate response relative to PSR (Figure 3.8). Therefore, the lumbar extension residual primarily contributed to the absolute level of corrected model metabolic cost instead of to the shape of the stroke rate response.

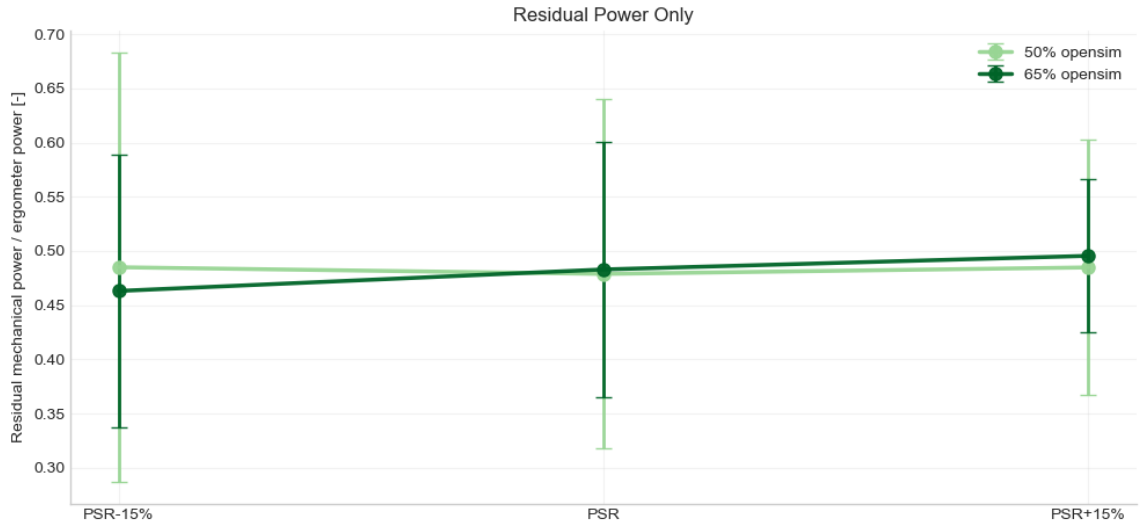

Figure 3.7: *Group mean residual mechanical power normalized by ergometer output power across stroke rate conditions. Residual mechanical power was not calculated by the Umberger2010 metabolic model but was added separately as a correction to account for mechanical power not represented in the muscle-only metabolic estimate. The relatively flat residual profile indicates that residual power mainly contributed to a vertical offset rather than explaining the stroke rate-dependent metabolic response.*

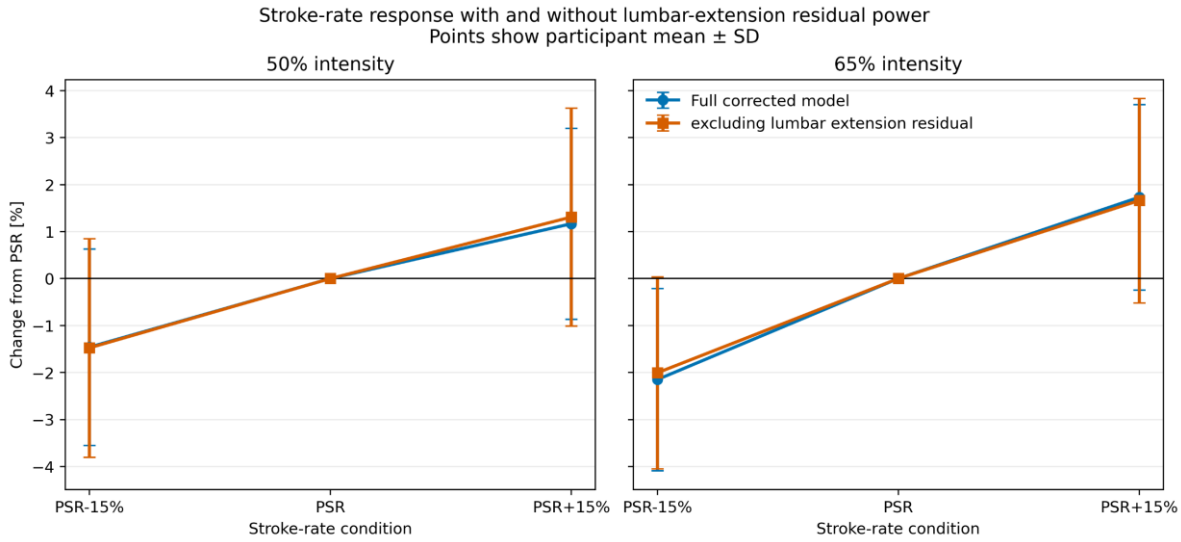

Figure 3.8: *Relative stroke rate response of the full residual-corrected model output and the output recalculated after excluding the absolute lumbar extension residual contribution. Values show the percentage change from PSR for the 50% and 65% intensity conditions. Points show group means and error bars indicate standard deviations across 12 participants. Excluding the lumbar extension residual had almost no effect on the predicted stroke rate response.*

3.2.5 Statistical Evaluation of Modelled Metabolic Cost and Model Error

To determine if the modelled metabolic cost showed effects of intensity and stroke rate, a repeated-measures ANOVA was performed on the metabolic predictions from the modelling workflow. The assumptions of the ANOVA were checked prior to the analysis. All twelve participants provided complete datasets across the six repeated measured conditions. None of the standardized residuals exceeded |3|, indicating no extreme outlier was present. However, Shapiro-Wilk tests on the residuals from the repeated measures indicated a significant deviation from normality ($W = 0.927, p < 0.001$). Therefore, the repeated measures ANOVA results were reported together with non-parametric sensitivity analyses using Friedman tests and Bonferroni-corrected Wilcoxon signed-rank comparisons within each intensity condition.

Analysis	Effect / comparison	Test statistic	p value	Effect size / direction	Interpretation
Shapiro–Wilk test	Repeated-measures residuals	$W = 0.927$	$p < 0.001$	—	Residuals deviated from normality
Repeated-measures ANOVA	Intensity	$F(1,11) = 270.26$	$p < 0.001$	$\eta_G^2 = 0.377$	Significant intensity effect
Repeated-measures ANOVA	Stroke rate	$F(2,22) = 14.33$	$p_{GG} < 0.001$	$\eta_G^2 = 0.017$	Significant stroke rate effect
Repeated-measures ANOVA	Intensity × stroke rate	$F(2,22) = 0.62$	$p_{GG} = 0.530$	$\eta_G^2 < 0.001$	No significant interaction
Friedman test	Stroke rate at 50% intensity	$Q = 6.50$	$p = 0.0388$	—	Significant stroke rate effect
Friedman test	Stroke rate at 65% intensity	$Q = 10.67$	$p = 0.0048$	—	Significant stroke rate effect
Wilcoxon signed-rank test	50%: PSR-15% vs PSR	$W = 22.0$	$p_{bonf} = 0.611$	—	Not significant
Wilcoxon signed-rank test	50%: PSR vs PSR+15%	$W = 17.0$	$p_{bonf} = 0.277$	—	Not significant
Wilcoxon signed-rank test	50%: PSR-15% vs PSR+15%	$W = 6.0$	$p_{bonf} = 0.0205$	—	Significant difference
Wilcoxon signed-rank test	65%: PSR-15% vs PSR	$W = 10.0$	$p_{bonf} = 0.0630$	—	Not significant after correction
Wilcoxon signed-rank test	65%: PSR vs PSR+15%	$W = 11.0$	$p_{bonf} = 0.0806$	—	Not significant after correction

Analysis	Effect / comparison	Test statistic	p value	Effect size / direction	Interpretation
Wilcoxon signed-rank test	65%: PSR-15% vs PSR+15%	$W = 0.0$	$p_{bonf} = 0.0015$	12/12 higher at PSR+15%	Significant difference

Table 3.2: *Statistical summary of the residual-corrected modelled normalized metabolic cost analysis. Repeated-measures ANOVA results are shown together with non-parametric Friedman and Wilcoxon signed-rank tests, because the repeated-measures residuals deviated from normality. Greenhouse-Geisser corrected p values are reported as p_{GG} for effects with more than two levels. Bonferroni-corrected post-hoc p values are reported as p_{bonf}.*

The statistical results are summarized in Table 3.2. The statistical analysis supports that normalized metabolic cost for rowing at an intensity of 65% was lower than that at an intensity of 50% and a gradual increase in cost with increasing stroke rate. There was no significant interaction between the intensity and stroke rate, indicating a similar stroke rate response at both intensities.

The Friedman tests also showed significant stroke rate effects within both intensity conditions. After Bonferroni correction, PSR+15% had a significantly higher modelled metabolic cost than PSR-15% at both intensities. The other pairwise comparisons were not significant. The model predicted a stroke rate effect, but this effect consisted of an increase from the PSR-15% to the PSR+15% stroke rate, instead of the experimental U-shaped response from deviations of the PSR.

To evaluate the agreement with the experimental data, model error was calculated as modelled normalized metabolic cost minus experimental normalized metabolic cost. The mean error was negative in all six conditions, indicating that the model underestimated the experimental metabolic cost. The repeated-measures ANOVA showed significant effects of intensity, stroke rate, and their interaction on model error. Underestimation was larger at 65% intensity, where mean errors ranged from -0.88 to -0.68, compared with -0.44 to -0.24 at 50% intensity.

No significant stroke rate effect was found using the Friedman test at 50% intensity. At 65% intensity, model error differed significantly between stroke rate conditions, with significantly less underestimation at PSR than at PSR-15%. The other pairwise comparisons were not significant after Bonferroni correction. These results show that the difference between modelled and experimental metabolic cost depended on both intensity and stroke rate. The model showed greater systematic underestimation at 65% intensity and did not reproduce the experimental stroke rate response.

3.3 Muscle-Level Musculoskeletal Simulation Results

3.3.1 Muscle-Group Metabolic Contributions

Seven muscle groups were analysed to determine which groups contributed most to the whole-body muscle metabolic estimate and how their contribution changes across stroke rates. Figure 3.9 displays the absolute metabolic contribution of each group, while Figure 3.10 displays its percentage contribution of the total modelled muscle metabolic power. Residual mechanical power was not included in this analysis, because it could not be assigned to individual muscles. The vasti showed the largest metabolic contribution across both intensities. Both their absolute and percentage contribution increased with stroke rate and was higher at 65% intensity compared to at 50% intensity. Other muscle groups also provided substantial contributions but showed smaller changes between stroke rate conditions.

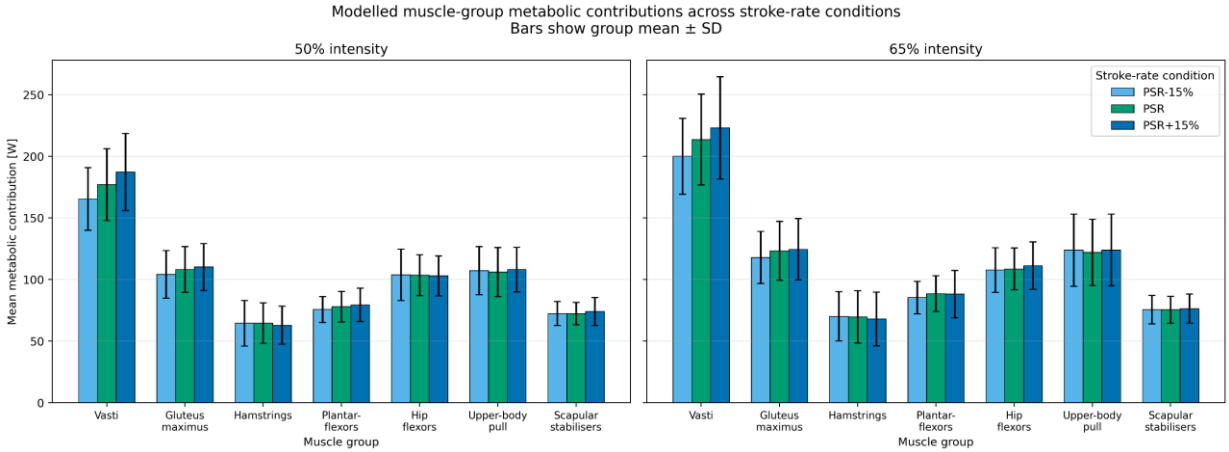

Figure 3.9: *Modelled muscle groups absolute metabolic contributions across stroke rate conditions. Bars show participant means and error bars show standard deviations across 12 participants.*

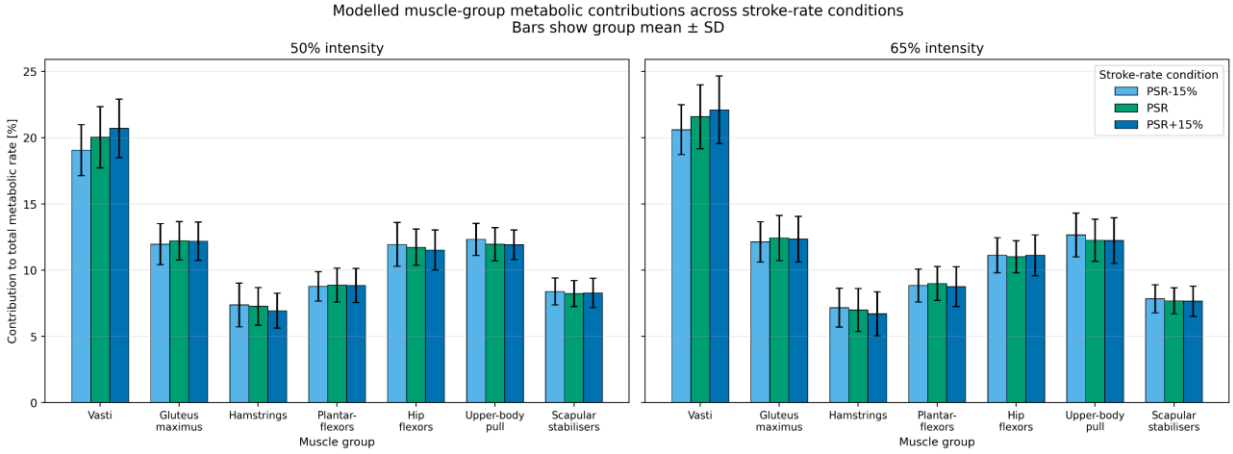

Figure 3.10: *Modelled muscle groups percentage metabolic contributions to the total modelled muscle metabolic power, across stroke rate conditions. Bars show participant means and error bars show standard deviations across 12 participants.*

3.3.2 Muscle-Group Activation

The mean muscle group activations predicted by SO are shown in Figure 3.11 and the peak activations are shown in Figure 3.12. Mean activations were generally higher at 65% intensity compared to 50% intensity. The vasti and gluteus maximus showed an increase in mean activation with increasing stroke rate, while other groups showed smaller changes between stroke rate conditions.

Peak activation showed a different response. The peak activation from the vasti, gluteus maximus, hamstrings and upper body pull muscle groups generally decreased as stroke rate increased. The other groups showed smaller changes between stroke rate conditions. Peak and mean activation both showed considerable variability between individuals. Statistical analyses of vasti peak activation and selected muscle-level outcomes are presented in Section 3.3.3.

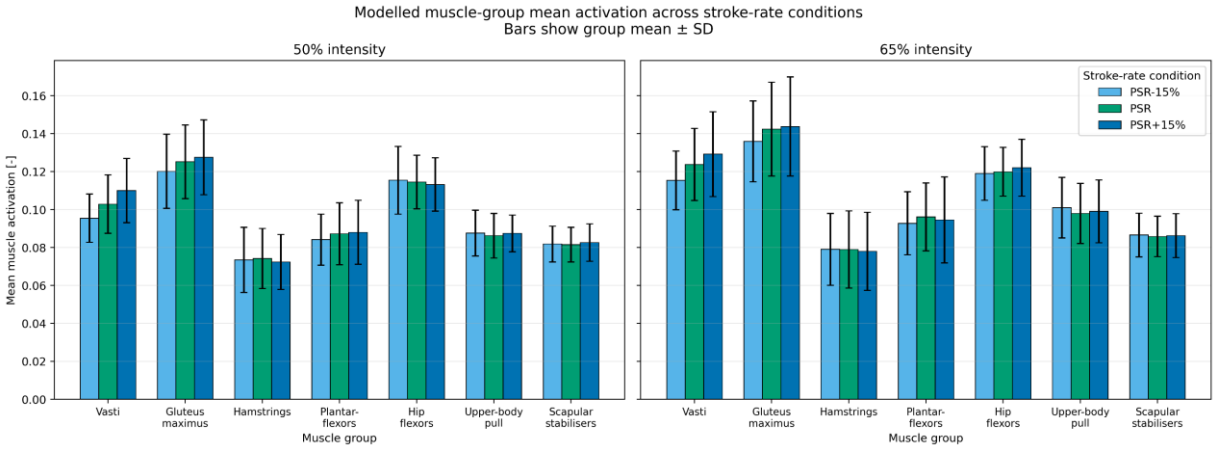

Figure 3.11: *Modelled muscle groups mean activation across stroke rate conditions. Bars show participant means and error bars show standard deviations across 12 participants.*

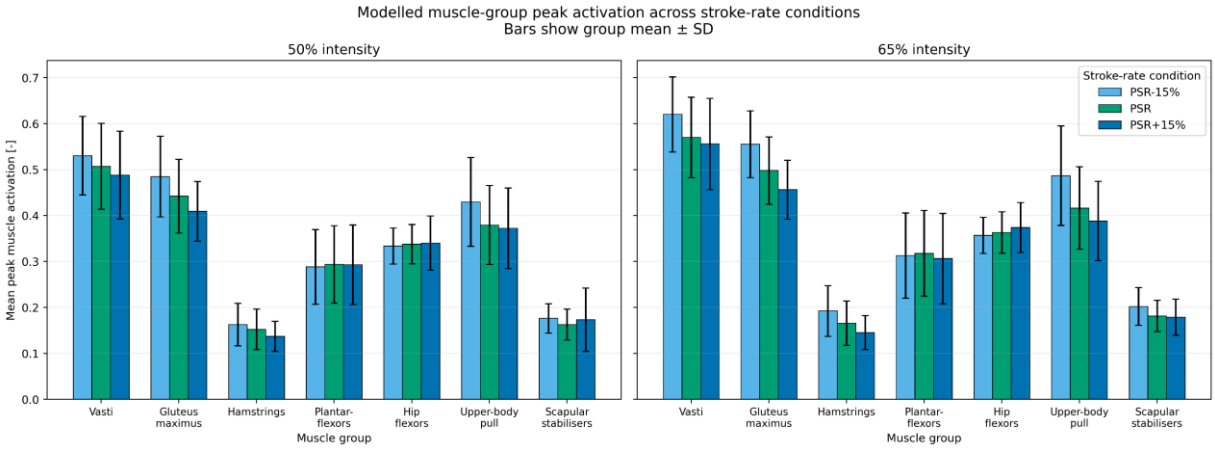

Figure 3.12: *Modelled muscle groups peak activation across stroke rate conditions. Bars show participant means and error bars show standard deviations across 12 participants.*

3.3.3 Statistical Evaluation of Selected Muscle-Level Outcomes

Statistical analyses were performed for the vasti peak activation, vasti absolute metabolic power, vasti summed activation squared and total summed activation squared. The vasti were chosen because they were the largest contributor to modelled muscle metabolic power. The squared activation figures are provided in Appendix D (see Figures D.1 and D.2), and the statistical results are found in Table 3.3.

As stroke rate increased, vasti peak activation decreased significantly, and vasti absolute metabolic power increased significantly. The non-parametric analyses confirmed stroke rate differences for both outcomes within each intensity. In contrast, neither vasti nor total summed activation squared showed a robust stroke rate effect. All four outcomes were significantly higher at 65% intensity, and none showed a significant interaction between intensity and stroke rate.

Outcome	Intensity effect	Stroke-rate effect	Interaction	Non-parametric result
Vasti summed activation squared	$F(1,11) = 133.44$, $p < 0.001$, $\eta_G^2 = 0.215$	$p_{GG} = 0.139$	$p_{GG} = 0.624$	Friedman significant at 50%, but no corrected pairwise comparison significant

Outcome	Intensity effect	Stroke-rate effect	Interaction	Non-parametric result
Total summed activation squared	$F(1,11) = 102.37$, $p < 0.001$, $\eta_G^2 = 0.250$	$p_{GG} = 0.458$	$p_{GG} = 0.397$	No significant Friedman or Wilcoxon results
Vasti peak activation	$F(1,11) = 99.68$, $p < 0.001$, $\eta_G^2 = 0.152$	$F(2,22) = 14.09$, $p_{GG} < 0.001$, $\eta_G^2 = 0.062$	$p_{GG} = 0.097$	Significant stroke-rate differences at both intensities
Vasti absolute metabolic power	$F(1,11) = 176.35$, $p < 0.001$, $\eta_G^2 = 0.242$	$F(2,22) = 19.25$, $p_{GG} < 0.001$, $\eta_G^2 = 0.078$	$p_{GG} = 0.807$	Significant stroke-rate differences at both intensities

Table 3.3: *Statistical analysis of selected vasti and whole-model muscle-level outcomes.*

3.3.4 Fibre Type Profile Sensitivity

The primary model analyses used the manually calibrated fibre type profile. To test the sensitivity of the metabolic prediction, the modelled metabolic cost was also estimated using a literature-based fibre type profile, described in Section 2.4.2. The comparison of both profiles with the experimental results can be seen in Figure 3.13.

The literature-based profile predicted a much lower normalized metabolic cost than the calibrated profile at both intensities and across all stroke rate conditions. Resulting in a considerably larger underestimation of the experimental metabolic cost from the literature-based profile compared to the manually calibrated profile.

By displaying how each dataset changed relative to its own PSR condition, it is shown that the fibre type profiles also affect the predicted stroke rate responses. At 50% intensity, the literature-based profile showed a smaller reduction from PSR to PSR-15% than the calibrated profile. The predicted increase at PSR+15% was similar. At 65% intensity, the relative responses produced by both profiles were similar. Both model configurations produced a decreasing metabolic cost when deviating from PSR to PSR-15% and therefore did not reproduce the experimental response, which showed the lowest group mean at or near PSR.

Overall, changing the fibre type profile strongly affected the absolute magnitude of the predicted metabolic cost and slightly affected the shape of the relative stroke rate response.

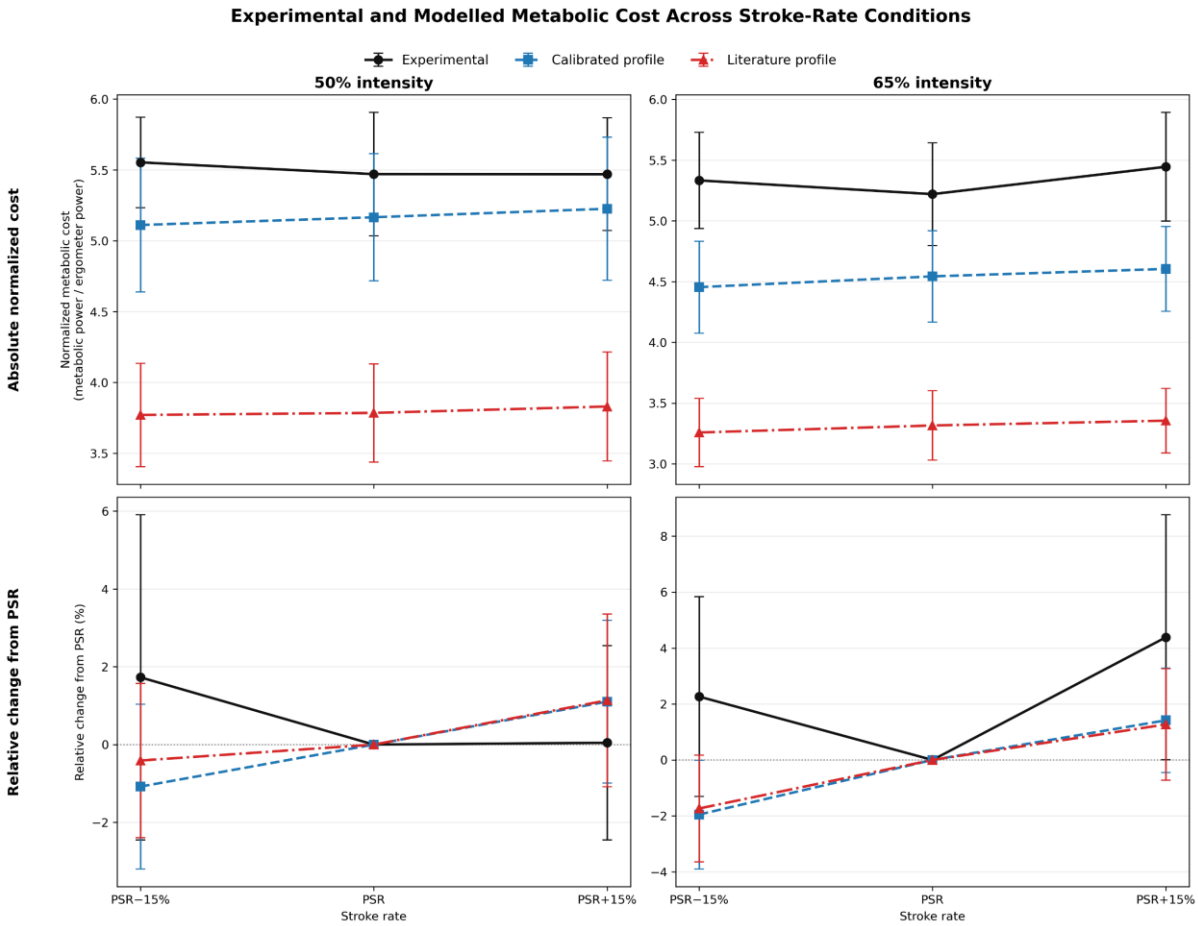

Figure 3.13: *Experimental and residual-corrected modelled normalized metabolic cost across stroke rate conditions using the manually calibrated and literature-based fibre type profiles. The upper panels show absolute normalized metabolic cost at 50% and 65% intensity. The lower panels show the relative change from the PSR condition.*

4 Discussion

4.1 Main Findings

This study investigated if metabolic efficiency may help explain why rowers select a preferred stroke rate (PSR) during submaximal ergometer rowing. The experimental results reveal a generally shallow U-shaped relationship between stroke rate and normalized metabolic cost. At PSR the metabolic cost was at or near lowest and increased when deviating from PSR. This effect was most apparent at 65% of 2K maximum power output, where PSR+15% resulted in a significant increase in metabolic cost compared to at PSR. At 50% intensity, the differences in metabolic cost were smaller and not statistically significant. Overall, these results suggest that metabolic efficiency may contribute to PSR selection, especially during higher power output.

Musculoskeletal modelling was used to explore if potential muscle-level mechanisms could explain why metabolic cost increased when deviating from PSR. The model reproduced the decrease in normalized metabolic cost from 50% intensity to 65% intensity but overestimated the improvement in efficiency. In addition, the model predicted a gradual increase from PSR-15% to PSR+15%, instead of the experimental stroke rate response where the metabolic cost was at or near lowest at PSR and the effect was stronger at 65% intensity. Residual mechanical power improved the absolute agreement between the modelled and experimental metabolic cost; however, the residual power remained relatively flat and therefore did not impact the modelled stroke rate response much.

The muscle-level results showed changes in metabolic contribution and activation across intensity and stroke rate conditions. The vasti group was the largest contributor to the modelled muscle metabolic power and their mean contribution increased with increasing stroke rate. In several groups the mean activation increased with increasing stroke rate, while the peak activation decreased with increasing stroke rate. While these findings provide insight into how the model distributed metabolic demands, they do not fully explain the experimentally observed metabolic minimum around PSR. Furthermore, changing the fibre type profile, from the manually calibrated to the literature-based profile, strongly affected the normalized metabolic prediction and slightly changed the modelled stroke rate response. This indicates that the model predictions depend on both assigned muscle properties and the estimated recruitment strategy, which may need to be personalized to improve the model and experimental agreement.

Overall, the experimental results support metabolic efficiency as a factor contributing to PSR selection, especially at higher intensity. The modelling workflow produced insight into how the muscle activation and metabolic demand were distributed across multiple muscle groups. However, because the model did not reproduce the experimentally observed stroke rate response, these muscle-level predictions should not be interpreted as the physiological cause of the increased metabolic cost when deviating from PSR. The fibre type profile sensitivity analysis indicates that personalizing fibre type may improve the agreement between modelled and experimental metabolic cost. Furthermore, improvements to the estimation of muscle recruitments, passive forces, and to the completeness of the musculoskeletal model may be required before the modelling workflow can explain the experimentally observed stroke rate response.

4.2 Experimental Stroke Rate Efficiency Response

The results of the study indicate that the relationship between normalized metabolic cost and stroke rate is shallow U-shaped across both intensities. The PSR selected by participants were the lowest or close to the lowest metabolic cost, regardless of intensity. Deviations from PSR resulted in increased metabolic demands. This effect was dependent upon intensity. For stroke rate changes at 50% power output there was only a slight and non-significant increase in metabolic costs. At 65% power output, the effect was clearer with a significant increase in metabolic cost at PSR+15%. The stroke rate deviations were somewhat asymmetric, especially at 50% intensity. The relative increase from PSR to PSR+15% was slightly larger at 50% intensity compared to 65% intensity, while the absolute increase was approximately 3.4 strokes/min at both intensities. Therefore, the greater metabolic penalty at 65% cannot be explained by a larger increase in absolute stroke rate. However, the differences between prescribed and measured stroke rate deviations should be considered when comparing the stroke rate responses between intensities.

This pattern suggests that the metabolic cost of increasing stroke rate becomes more important as external power output increases. At a higher stroke rate, each stroke is performed quicker, increasing the contraction frequency and the rate at which body segments are accelerated and decelerated. While rowing at a greater stroke rate may allow for a reduction in the amount of force needed per stroke, given a specific power output, this will also require a greater amount of internal work and neuromuscular cost to perform the more frequent rate [2], [16], [17]. The 65% condition likely moved participants closer to this trade-off, making the high stroke rate penalty more visible.

The difference of stroke rate response between intensities may indicate that rowers had more flexibility in how they produced the required power at 50% intensity. At 50% intensity, different combinations of muscle recruitment, activation timing and rowing technique may achieve the required power output with similar whole-body metabolic costs. At 65% intensity and PSR+15%, the combination of greater power demand and shorter available stroke time may decrease the flexibility of effective coordination strategies. Deviations from a more efficient movement pattern may therefore have been more difficult to compensate for and more metabolically costly.

This interpretation is consistent with cycling literature, which is also a cyclic movement sport like rowing. Research indicates that movement frequency affects metabolic efficiency both from mechanical and physiological mechanisms [2], [16], [18]. At low movement frequency, the higher force required per cycle increases the fibre stress and may increase the recruitment of less efficient type II fibres [3], [18]. In contrast, when using high movement frequencies repeated muscle activations, transporting ions, as well as internal work can increase oxygen uptake and thus metabolic cost [2], [16], [19]. Therefore, while rowing and cycling are fundamentally different activities because the trunk and upper body are moving substantially during rowing compared to cycling, both require generating cyclic forces to produce a power output. Thus, providing an opportunity to use the mechanical and physiological mechanisms from cycling to help understand the results of this study related to rowing.

From a practical rowing perspective, these findings suggest that the PSR may reflect a metabolically favourable stroke rate for a given power output. This was most apparent at 65% intensity, where rowing at PSR+15% showed a significant increase in normalized metabolic cost compared to rowing at PSR. However, these findings should not be interpreted as evidence that higher stroke rates are

always less efficient than the PSR. Higher stroke rates may still be required to achieve higher power outputs during racing or high-intensity training. Instead, these results suggest that when power output is constant, rowing at a higher stroke rate than PSR could increase the metabolic cost, especially at 65% of 2K max power output. At lower intensity, stroke rate may be less influential, since deviations from PSR produced only small non-significant changes in normalized metabolic cost at 50% of 2K max power output. Additionally, these results were obtained during ergometer rowing and the relationship between stroke rate and efficiency may differ during on-water rowing, because of boat dynamics and crew synchronization.

4.3 Modelled Muscle-Level Responses

The muscle-level analysis showed how the model distributed the metabolic demand across muscle groups. The largest contributor to the modelled muscle metabolic cost at both intensities was the vasti muscle group. Both absolute and relative metabolic contribution of the vasti group increased with increasing stroke rate, indicating a larger modelled metabolic contribution from the knee extensors at higher stroke rate. Other muscle groups showed smaller changes across stroke rates.

The vasti results showed opposing stroke rate responses in peak activation and metabolic power. Peak vasti activation decreased as stroke rate increased, while vasti metabolic power increased. This suggests a possible trade-off between greater peak vasti activation, indicating greater instantaneous muscle demand, at slower stroke rates and greater vasti metabolic demand at faster stroke rates. Selected PSR may lie between these opposing demands.

Neither vasti nor total summed activation squared showed a robust stroke rate effect. Therefore, the increase in metabolic power of the vasti at higher stroke rates cannot simply be explained by an increase in the squared activation objective minimized by Static Optimization (SO). Changes in fibre length, contraction velocity, mechanical work and heat production components of the Umberger2010 model may also have contributed.

The increased mean activation and metabolic contribution of the vasti may help explain the gradual increase in metabolic cost from PSR-15% to PSR+15% predicted by the model and could represent a component of the corresponding experimental increase. However, the model predicted a small and similar increase at both intensities and did not capture the larger penalty observed experimentally at 65% intensity or the experimental metabolic increase at PSR-15%. The muscle-level results may identify part of the metabolic demand associated with higher intensity and stroke rate, but they do not provide a complete explanation for the stroke rate response when deviating from PSR.

4.4 Whole-Body Model Performance and Stroke Rate Mismatch

The modelling workflow reproduced some characteristics of the experimental results but also failed to capture some of the experimental metabolic trends. The model predicted lower normalized metabolic cost at 65% intensity compared to 50% intensity, which is consistent with the experimental result that metabolic cost per Watt of ergometer output decreased at 65% intensity compared to at 50% intensity. However, the model predicted a larger magnitude of this decrease than seen in the experimental results. At PSR, the model predicted approximately a 12% decrease in normalized metabolic cost from the 50% to the 65% intensity condition, whereas the experimental decrease was

only about 4.6%. This indicates that the model overestimated the improvement in efficiency at the 65% intensity condition.

While the model did predict a significant stroke rate effect, the shape of the response from the model differed from the experimental results. The model predicted normalized metabolic cost that gradually increased from PSR-15% to PSR+15% at both intensities, and there was no significant interaction between stroke rate and intensity. In contrast the experimental results showed a shallow U-shaped response around PSR and a stronger increase at PSR+15% during the 65% intensity condition compared to the 50% intensity condition. Thus, the model captured a small increase in metabolic cost at PSR+15% but failed to reproduce the higher metabolic cost at PSR-15% or the stronger metabolic penalty at 65% intensity.

The mismatch between the experimental and modelled metabolic data suggests that the modelling workflow may not fully represent the physiological costs associated with changes in stroke rate and intensity. SO minimizes muscle activations independently at each time step and does not account for activation history or contraction dynamics [20]. It may also underestimate antagonist activity, co-contraction and additional activation required for trunk and pelvis stabilization [21], [22], [23]. Furthermore, the rigid tendon assumption used in SO may be especially relevant for rowing because the movement involves large ranges of motion throughout the stroke, particularly at the hip and pelvis. These movements can produce substantial changes in muscle tendon unit length, for example in the gluteal muscles around the catch. In vivo, compliant tendons may stretch under load and store and release elastic energy, potentially reducing the active muscle force and activation required during parts of the stroke. Modelling these elastic contributions could strongly affect the predicted muscle activations, fibre mechanics and metabolic cost. Arones et al. [24] showed that how muscle activations are generated and the level of musculoskeletal personalization influenced the estimate of metabolic cost. In their comparison, differences in SO and EMG-driven activation patterns resulted in different metabolic cost estimations by the Umberger2010 model.

In previous gait simulations it is shown that metabolic energy models can reproduce condition dependent trends, but that the magnitude and scaling of metabolic cost depend on the selected modelling and recruitment assumptions [25]. In addition, breathing gas measurements include whole-body costs, such as respiratory muscle work, that are absent in the model estimate [26]. These limitations may be particularly relevant when stroke rate increases because activation-relaxation cycles occur more frequently. Therefore, the predicted activations could be mechanically valid, but too economical physiologically, contributing to both the larger underestimation at 65% intensity and the mismatch in the stroke rate response.

4.5 Fibre Type Sensitivity and Model Personalization

The fibre type sensitivity analysis showed that the assigned muscle fibre type compositions had a large impact on the normalized metabolic cost predicted by the model. The literature-based profile produced considerably lower metabolic costs compared to the manually calibrated profile and therefore increased the underestimation compared to experimental results at both intensities. The relatively close absolute agreement between the calibrated profile and the experimental results should not be interpreted as independent validation, because this profile was adjusted using the experimental results at 50% intensity.

Changing the fibre type profile also caused a small change in the relative stroke rate response, particularly at 50% intensity. This indicates that fibre type assumptions can affect not only the absolute magnitude of the prediction, but also the shape of the predicted metabolic cost curve. However, both profiles did not reproduce the experimental shallow U-shaped curve and their relative responses remained similar at 65% intensity. Therefore, fibre type composition alone does not explain the mismatch between the modelled and experimental results.

Because fibre type composition was not measured in the participants, both profiles assign assumed compositions instead of the actual compositions. Participant personalized fibre type profiles based on physiological measurements could potentially improve individual metabolic predictions and as a result also group-level metabolic prediction. However changing fibre type composition only changes energetic cost assigned to the activations predicted by SO, not the activation patterns themselves. A more accurate modelling workflow may therefore require personalization of both muscle properties and recruitment behaviour.

4.6 Residual Mechanical Power and Model Completeness

The numerical agreement between the modelled and experimental metabolic cost was increased by the inclusion of residual mechanical power. This is shown in the scatter plot comparisons (see Figures 3.4 and 3.5), where the residual-corrected prediction data points are closer to the identity line than without residual-correction. This should not be interpreted as a direct physiological metabolic estimate but rather as a correction of the model-experimental differences. The Umberger2010 Model [11] does not produce a residual power value by itself, but the residual power was added independently to account for the lack of representation of mechanical power in the muscle-only model estimate.

The residual power was relatively constant across stroke rate and intensity conditions; therefore, the residual power served primarily as a vertical offset to the modelled metabolic cost, instead of an explanation for the experimentally observed stroke rate dependent responses. These results support the interpretation that residual corrections can reduce the absolute underestimation, but do not provide any explanation for the increase of metabolic cost at PSR+15% at the 65% intensity condition.

The lumbar extension actuator made up about 50% of the total residual correction, supporting the interpretation that the simplified trunk representation omitted a considerable portion of the mechanical demand. However, its contribution had little effect on the stroke rate response. Because trunk muscles contribute to stability and force transfer during rowing, part of the mechanical demand from missing or simplified trunk mechanics in the model [21], [23] may have been redistributed to adjacent muscle groups.

As a result, residual power should be interpreted with caution. Residual powers were calculated separately from the Umberger2010 muscle metabolic calculations and reflect mechanical demands that were not fully generated by modelled muscles, because muscles are missing in the model or the modelled muscles produce insufficient force. However, this residual-correction only represents mechanical power. It does not represent the physiological cost that modelled muscles would require to produce this power, such as activation heat, maintenance heat, shortening heat, or fibre dependent metabolic effects included in the Umberger2010 metabolic probe. Therefore, the residual-correction

estimate is a useful correction for mechanical power missing from the muscle-only metabolic simulation, but it should not be interpreted as a direct physiological output of the metabolic model.

4.7 Limitations

Several limitations should be considered when interpreting these results. The first limitation is that the experimental metabolic data were obtained from breathing gas analysis and represent a measure of whole-body metabolic cost instead of isolated muscle metabolic cost. There could also be small measurement errors in the breathing gas data. The final metabolic calculations removed the contribution of the basal metabolic rate to both the experimental and modelled data, but the experimental measurements may still include physiological costs that are not represented by the model, such as respiratory muscle work [26].

Second, the modelling workflow relies strongly on the muscle activation patterns provided by SO. Since SO determines muscle recruitment at each time step independently and assumes rigid tendons, it does not fully represent activation history, tendon compliance or stabilizing co-activation [20], [22]. This limits the ability of the model to reflect physiological recruitment strategies. Furthermore, there were simplifications in the modelling process that could impact how well the model represented trunk mechanics during rowing, such as a rigid spine and no modelled erector spinae muscle. Residual mechanical power partly accounted for missing mechanical demand but did not represent physiological metabolic cost.

Third, several participant-specific muscle properties, such as fibre type composition and maximum muscle forces, were not measured directly. The primary fibre type profile was manually calibrated using the group experimental metabolic data at 50% intensity. Consequently, the agreement at 50% intensity should not be interpreted as validation. The literature-based profile was physiologically supported but remained a generic assumption instead of a direct measure of actual fibre type compositions of each participant.

Finally, the study involved complete data of twelve male experienced rowers and only three stroke rates for each intensity. This limitation reduced the ability to determine if PSR was the actual metabolic optimal stroke rate or part of a wider metabolically favourable range and it limits generalization to other populations and on-water rowing. Most muscle-group analyses were descriptive, while inferential analyses were limited to selected vasti and whole-model outcomes. The remaining muscle-group patterns should therefore be interpreted cautiously.

4.8 Future Work

Future experimental work should further investigate the relationship between stroke rate and efficiency with a larger sample size, larger stroke rate deviations and more diverse samples. In the present study the group means show a shallow U-shaped relationship around PSR, but only the increase from PSR to PSR+15% at 65% intensity was statistically significant. A larger sample size would provide for a higher probability to detect smaller effects, particularly at 50% intensity and for the PSR-15% condition. Additional stroke rates would be valuable to establishing whether the metabolic optimum occurs at or close to PSR or if there is a metabolically favourable range for an individual.

Future modelling work should further personalize the musculoskeletal models. Participant-specific fibre type composition and muscle strength could be measured or estimated directly instead of assigning generic profiles. The sensitivity analysis showed that fibre type assumptions affected both the magnitude and slightly the shape of the metabolic prediction across stroke rates. The measured EMG data could be used to compare changes in activation between intensities and stroke rates, instead of only validating activation timing [6].

The modelling workflow could also be improved by using a more complete trunk model with lumbar muscles and by applying recruitment methods that represent activation dynamics, passive forces and co-contraction. The use of approaches such as the Rapid Muscle Redundancy solver, dynamic optimization, or EMG driven modelling to create muscle activations may produce more realistic activation patterns than Static Optimization. These improvements should be evaluated by determining if they improve both the absolute metabolic prediction and the predicted metabolic response to deviations from PSR.

5 Conclusion

This thesis investigated if deviations from the preferred stroke rate affect metabolic efficiency during submaximal ergometer rowing and if this effect depends on intensity. The experimental results showed that PSR was at or near the lowest normalized metabolic cost at group level. Deviations from PSR produced small and nonsignificant changes at 50% of 2K maximum ergometer power. At 65% intensity, however, PSR+15% resulted in a significant increase in metabolic cost compared to PSR. The effect of stroke rate on metabolic efficiency is dependent on intensity and was clearest at higher submaximal workload.

These results support metabolic efficiency as a factor that influences preferred stroke rate selection. However, the shallow metabolic response across stroke rates and the variability between participants suggest that PSR generally lies within a metabolically favourable range instead of a precise metabolic optimum. Additional variables, such as technique, local muscular demand, fatigue and individual physiology may also contribute to PSR selection.

The musculoskeletal model reproduced the lower normalized metabolic cost at 65% intensity compared to 50% intensity, but modelled metabolic cost increased gradually from PSR-15% to PSR+15% at both intensities instead of reproducing the experimental shallow U-shaped curve and a stronger PSR+15% metabolic penalty at 65% intensity. Residual mechanical power improved the absolute agreement between modelled and experimental metabolic cost but mainly acted as a vertical correction and did not account for the stroke rate dependent response.

The muscle-level analysis showed that the vasti contributed the most to the muscle metabolic power produced by the model and that their contribution and mean activation increased with increasing stroke rate, while peak activation decreased for several muscle groups. This may indicate a trade-off between greater peak muscle demand at slower stroke rates and greater modelled metabolic demand at faster stroke rates. However, neither vasti nor total summed activation squared showed a robust stroke rate effect, indicating that the increase in vasti metabolic power was not simply driven by the squared activation objective minimized by Static Optimization. These activation patterns should only be interpreted as predictions of the model instead of actual physiological mechanisms. The fibre type sensitivity analysis further demonstrated that the assumed muscle properties had a large effect on the absolute metabolic prediction and a small effect on the stroke rate response. Therefore, participant personalized muscle properties may improve metabolic predictions. Improved recruitment estimation and a more complete musculoskeletal model are also required before the modelling workflow can reliably explain why a rower selects a preferred stroke rate.

The hypotheses were partly supported by the analysis. Normalized metabolic cost was lowest or close to lowest at PSR, although the only statistically significant difference was between PSR and PSR+15% at 65% intensity. The findings supported the hypothesis of a significant interaction between stroke rate and efficiency. However, the modelling hypothesis was not supported, because the model did not reproduce the experimental stroke rate response, and neither vasti nor total summed activation squared showed a clear minimum at PSR.

Bibliography

[1] I. Hunter, K. Lee, J. Ward, and J. Tracy, “Self-optimization of stride length among experienced and inexperienced runners,” Int. J. Exerc. Sci., vol. 10, no. 3, pp. 446–453, 2017, doi: 10.70252/LSDP6161.

[2] T. Takaishi, Y. Yasuda, T. Ono, and T. Moritani, ‘Optimal pedaling rate estimated from neuromuscular fatigue for cyclists’, *Med. Sci. Sports Exerc.*, vol. 28, no. 12, pp. 1492–1497, Dec. 1996, doi: 10.1097/00005768-199612000-00008.

[3] E. A. Hansen, J. L. Andersen, J. S. Nielsen, and G. Sjøgaard, ‘Muscle fibre type, efficiency, and mechanical optima affect freely chosen pedal rate during cycling’, *Acta Physiol. Scand.*, vol. 176, no. 3, pp. 185–194, 2002, doi: 10.1046/J.1365-201X.2002.01032.X.

[4] M. J. Hofmijster, A. J. Van Soest, and J. J. De Koning, ‘Gross efficiency during rowing is not affected by stroke rate’, *Med. Sci. Sports Exerc.*, vol. 41, no. 5, pp. 1088–1095, May 2009, doi: 10.1249/MSS.0B013E3181912272.

[5] G. Ettema, A. Haug, T. P. Ludvigsen, and J. Danielsen, ‘The role of stroke rate and intensity on rowing technique’, *Sports Biomech.*, vol. 24, no. 10, pp. 2931–2952, Oct. 2025, doi: 10.1080/14763141.2022.2135457.

[6] S. V. Loose, “Relative muscle contributions to mechanical work in ergometer rowing: Experiment, modeling, and analysis,” M.Sc. thesis, Faculty of Mechanical Engineering, Delft University of Technology, Delft, The Netherlands, 2025.

[7] S. D. Uhlrich, R. W. Jackson, A. Seth, J. A. Kolesar, and S. L. Delp, ‘Muscle coordination retraining inspired by musculoskeletal simulations reduces knee contact force’, *Sci. Rep.*, vol. 12, no. 1, Dec. 2022, doi: 10.1038/S41598-022-13386-9.

[8] A. Seth, M. Dong, R. Matias, and S. Delp, ‘Muscle contributions to upper-extremity movement and work from a musculoskeletal model of the human shoulder’, *Front. Neurorobot.*, vol. 13, 2019, doi: 10.3389/FNBOT.2019.00090.

[9] A. Seth *et al.*, ‘OpenSim: Simulating musculoskeletal dynamics and neuromuscular control to study human and animal movement’, *PLoS Comput. Biol.*, vol. 14, no. 7, p. e1006223, Jul. 2018, doi: 10.1371/JOURNAL.PCBI.1006223.

[10] S. L. Delp *et al.*, ‘OpenSim: Open-source software to create and analyze dynamic simulations of movement’, *IEEE Trans. Biomed. Eng.*, vol. 54, no. 11, pp. 1940–1950, Nov. 2007, doi: 10.1109/TBME.2007.901024.

[11] B. R. Umberger, ‘Stance and swing phase costs in human walking’, *J. R. Soc. Interface*, vol. 7, no. 50, pp. 1329–1340, Sep. 2010, doi: 10.1098/RSIF.2010.0084.

[12] Z. H. He, R. Bottinelli, M. A. Pellegrino, M. A. Ferenczi, and C. Reggiani, ‘ATP consumption and efficiency of human single muscle fibers with different myosin isoform composition’, *Biophys. J.*, vol. 79, no. 2, pp. 945–961, 2000, doi: 10.1016/S0006-3495(00)76349-1.

[13] L. J. Bhargava, M. G. Pandy, and F. C. Anderson, ‘A phenomenological model for estimating metabolic energy consumption in muscle contraction’, *J. Biomech.*, vol. 37, no. 1, pp. 81–88, Jan. 2004, doi: 10.1016/S0021-9290(03)00239-2.

[14] M. A. Johnson, J. Polgar, D. Weightman, and D. Appleton, ‘Data on the distribution of fibre types in thirty-six human muscles: An autopsy study’, *J. Neurol. Sci.*, vol. 18, no. 1, pp. 111–129, Jan. 1973, doi: 10.1016/0022-510X(73)90023-3.

[15] J. M. Steinacker, “Physiological aspects of training in rowing,” Int. J. Sports Med., vol. 14, suppl. 1, pp. S3–S10, Sep. 1993.

[16] M. Tokui and K. Hirakoba, ‘Estimation of oxygen cost of internal power during cycling exercise with changing pedal rate’, *J. Physiol. Anthropol.*, vol. 27, no. 3, pp. 133–138, 2008, doi: 10.2114/JPA2.27.133.

[17] S. F. Brennan, A. G. Cresswell, D. J. Farris, and G. A. Lichtwark, ‘The Effect of Cadence on the Mechanics and Energetics of Constant Power Cycling’, *Med. Sci. Sports Exerc.*, vol. 51, no. 5, pp. 941–950, May 2019, doi: 10.1249/MSS.0000000000001863.

[18] L. E. Ahlquist, D. R. Bassett, R. Sufit, F. J. Nagle, and D. P. Thomas, ‘The effect of pedaling frequency on glycogen depletion rates in type I and type II quadriceps muscle fibers during submaximal cycling exercise’, *Eur. J. Appl. Physiol. Occup. Physiol.*, vol. 65, no. 4, pp. 360–364, Jul. 1992, doi: 10.1007/BF00868141.

[19] J. A. Zoladz, K. Duda, J. Majerczak, and P. Thor, ‘Effect of different cycling frequencies during incremental exercise on the venous plasma potassium concentration in humans’, *Physiol. Res.*, vol. 51, no. 6, pp. 581–586, 2002, doi: 10.33549/PHYSIOLRES.930262.

[20] F. C. Anderson and M. G. Pandy, ‘Static and dynamic optimization solutions for gait are practically equivalent’, *J. Biomech.*, vol. 34, no. 2, pp. 153–161, 2001, doi: 10.1016/S0021-9290(00)00155-X.

[21] M. Yamashita *et al.*, ‘Trunk Muscle Activities during Ergometer Rowing in Rowers with and without Low Back Pain’, *J. Sports Sci. Med.*, vol. 22, no. 2, pp. 338–344, Jun. 2023, doi: 10.52082/JSSM.2023.338.

[22] A. Kian *et al.*, ‘Static optimization underestimates antagonist muscle activity at the glenohumeral joint: A musculoskeletal modeling study’, *J. Biomech.*, vol. 97, Dec. 2019, doi: 10.1016/J.JBIOMECH.2019.109348.

[23] R. Hammami *et al.*, ‘Effects of global versus local trunk muscle strength training on muscle strength, proxies of power and rowing-specific performance in pubertal male rowers’, *PLoS One*, vol. 21, no. 2, p. e0343291, Feb. 2026, doi: 10.1371/JOURNAL.PONE.0343291.

[24] M. M. Arones, M. S. Shourijeh, C. Patten, and B. J. Fregly, ‘Musculoskeletal Model Personalization Affects Metabolic Cost Estimates for Walking’, *Front. Bioeng. Biotechnol.*, vol. 8, p. 588925, Nov. 2020, doi: 10.3389/FBIOE.2020.588925.

[25] A. D. Koelewijn, D. Heinrich, and A. J. van den Bogert, ‘Metabolic cost calculations of gait using musculoskeletal energy models, a comparison study’, *PLoS One*, vol. 14, no. 9, p. e0222037, Sep. 2019, doi: 10.1371/JOURNAL.PONE.0222037.

[26] A. Aliverti, ‘The respiratory muscles during exercise’, *Breathe*, vol. 12, no. 2, pp. 165–168, Jun. 2016, doi: 10.1183/20734735.008116.

AI Acknowledgement

I acknowledge the use of ChatGPT to support the development of this thesis by providing writing feedback, assisting with programming/debugging, and generating a schematic figure (Figure 1.1) and the title page background. The research design, data analysis, result interpretation, and the final text was made and written by the author.

Appendix A: Umberger2010 Metabolic Probe Settings

This Appendix shows the settings for the Umberger2010 metabolic probe in the code of the musculoskeletal models.

Code:

```
<Umberger2010MuscleMetabolicsProbe name="metabolic_cost_analysis">
   <activation_maintenance_rate_on>true</activation_maintenance_rate_on>
   <shortening_rate_on>true</shortening_rate_on>
   <basal_rate_on>false</basal_rate_on>
   <mechanical_work_rate_on>true</mechanical_work_rate_on>
   <use_Bhargava_recruitment_model>true</use_Bhargava_recruitment_model>
   <include_negative_mechanical_work>true</include_negative_mechanical_work>
   <report_total_metabolics_only>false</report_total_metabolics_only>
```

Appendix B: Manually Calibrated and Literature-Based Rower Profile Fibre Type Compositions

Fibre-type group	Included muscle patterns	Calibrated type I (%)	Literature type I (%)
Deep postural	soleus, tibpost, fdl, fhl	40	70
Primary engines	vasint, vaslat, vasmed	40	70
Power movers	glmax, latissimus dorsi, teres major, deltoid	30	70
Scapular stability	trapezius, serratus anterior, rhomboid, levator scapulae	40	60
Hip/ankle stability	gluteus medius/minimus, piri, psoas, iliacus, tibant, peroneals, edl, ehl	40	60
Hybrid movers	adductors, gracilis, sartorius, gastrocnemius, pectoralis, rotator-cuff muscles	30	60
Fast dynamic	hamstrings, rectus femoris, TFL	30	50
Arms finish	biceps, triceps, brachialis, coracobrachialis	30	50

Table B.1: *Assigned type I fibre percentages for the manually calibrated and literature-based fibre type profiles.*

Appendix C: Muscle Groups Used for the Muscle-Level Analysis

Muscle group:	OpenSim muscle-name patterns:
Vasti	vasint, vaslat, vasmed
Gluteus maximus	glmax1, glmax2, glmax3
Hamstrings	bflh, bfsh, semimem, semiten
Plantar flexors	gaslat, gasmed, soleus
Hip flexors	iliacus, psoas, recfem, sart, tfl
Upper-body pulling muscles	latissimusdorsi, teresmajor, bic_long, bic_brevis, bra
Scapular stabilisers	trapeziusscapula, trapeziusclavicle, rhomboideus, serratusanterior, levatorscapulae

Table C.1: *Muscle elements included in each functional muscle group used for the muscle-level analysis.*

Appendix D: Squared-Activation Analyses

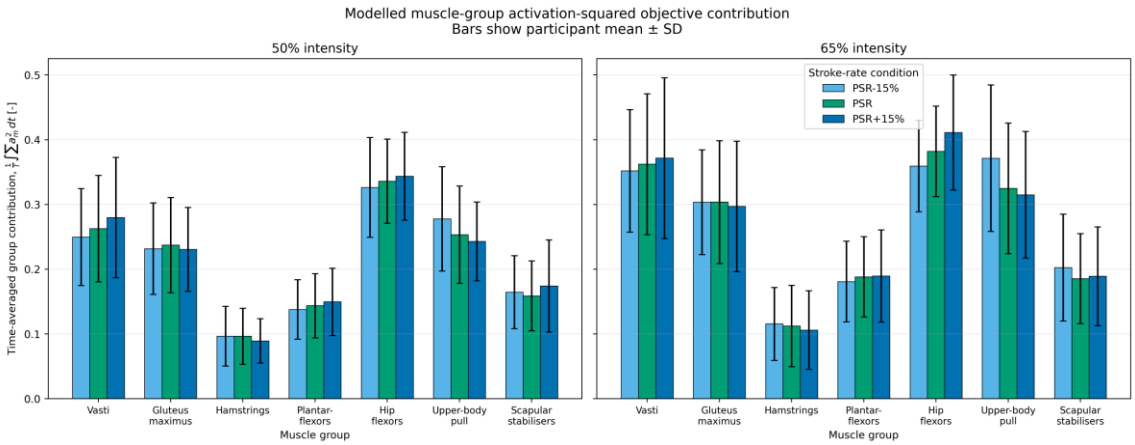

Figure D.1: *Time-averaged summed squared activation for each functional muscle group at 50% and 65% intensity. Bars show the group mean and error bars show the standard deviation across 12 participants. Values represent the summed squared activations of all muscle elements assigned to each group. Therefore, comparisons between groups are partly influenced by the number of muscle elements included in each group.*

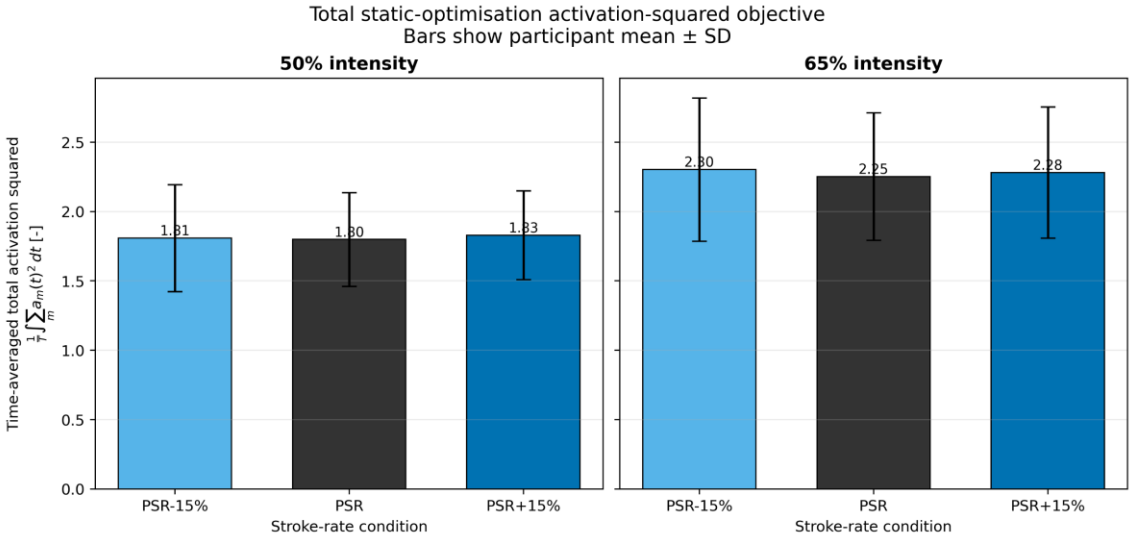

Figure D.2: *Total time-averaged summed squared activation across all model muscle elements at PSR−15%, PSR and PSR+15% for the 50% and 65% intensity conditions. Bars show the group mean and error bars show the standard deviation across 12 participants.*

Appendix E: Individual Experimental and Modelled Metabolic Responses

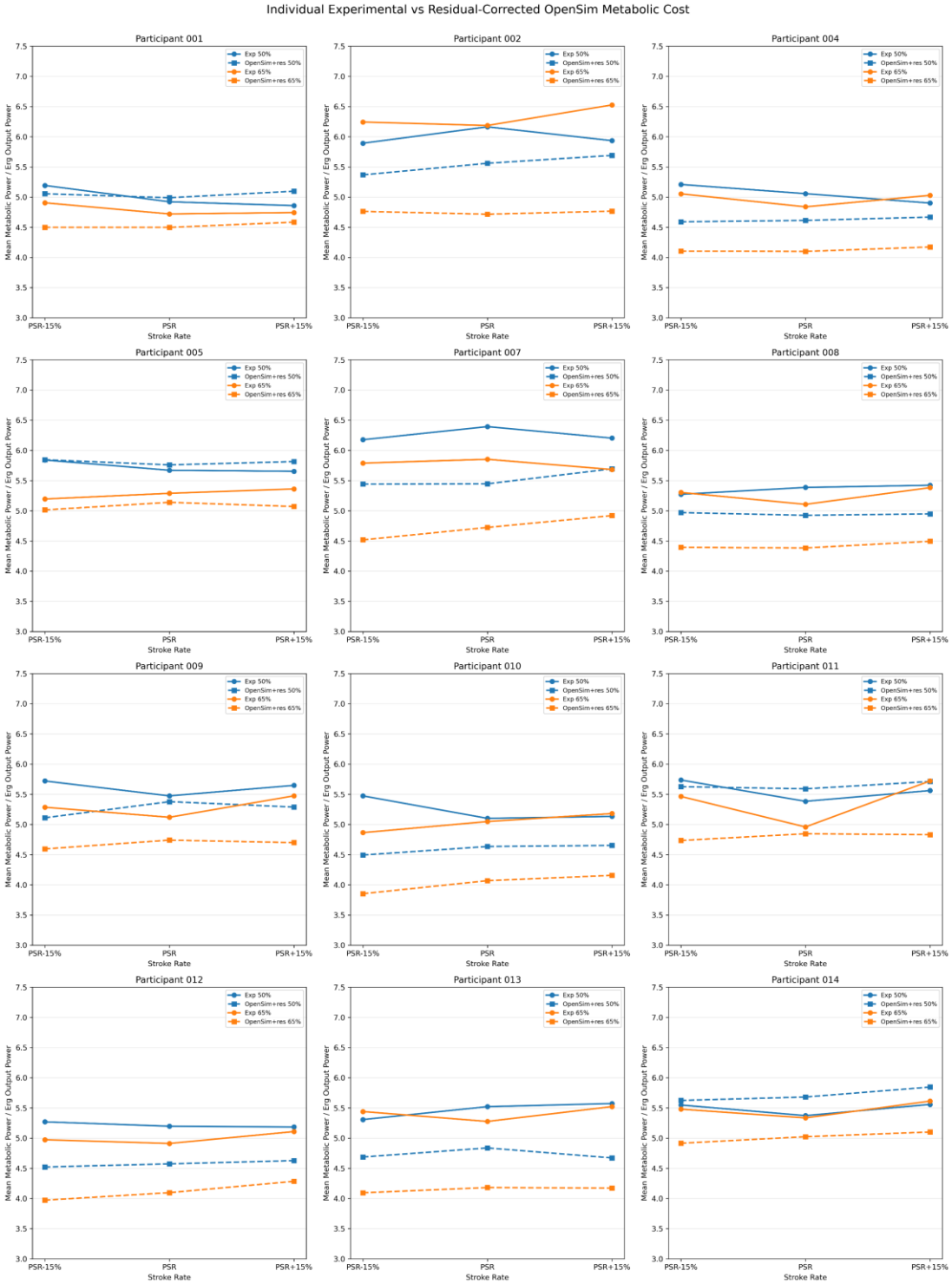

Figure E.1: *Overlay of Individual residual-corrected OpenSim and experimental participant profiles showing the normalized metabolic cost across the three stroke rate conditions (PSR-15%, PSR, and PSR+15%). Each panel represents one participant and compares the experimental breathing gas response with the modelled prediction for the 50% and 65% intensity conditions.*